



Universidad Autónoma
de Madrid

Biblos-e Archivo
Repositorio Institucional UAM

Repositorio Institucional de la Universidad Autónoma de Madrid

<https://repositorio.uam.es>

Esta es la **versión de autor** del artículo publicado en:
This is an **author produced version** of a paper published in:

Journal of Physics Condensed Matter 33.42 (2021): 425604

DOI: <https://doi.org/10.1088/1361-648X/ac1155>

Copyright: © 2021 IOP Publishing Ltd.

El acceso a la versión del editor puede requerir la suscripción del recurso
Access to the published version may require subscription

A Local-Orbital Density Functional formalism for a many-body atomic Hamiltonian: Hubbard-Hund's Coupling and DFT+U functional

Diego Soler-Polo, José Ortega, and Fernando Flores

*Departamento de Física Teórica de la Materia Condensada and
Condensed Matter Physics Center (IFIMAC), Facultad de Ciencias,
Universidad Autónoma de Madrid, E-28049 Madrid, Spain*

(Dated: July 2, 2021)

Abstract

In the conventional DFT+U approach, the mean field solution of the Hubbard Hamiltonian associated with the d or f ($i\sigma$) electrons of a transition metal atom is used to define the DFT+U potential acting on the $i\sigma$ -electrons. In this work, we go beyond that mean field solution by analyzing the correlation energy and potential for a multi-level atom described by a Kanamori Hamiltonian connected to different channels representing the environment. As a first step, we analyze the many-body solution of our model, using a local-orbital Density Functional formalism that takes as independent variables the orbital occupancies, $n_{i\sigma}$, of the atomic orbitals; accordingly, we present the corresponding Density Functional solution describing the correlation energy and potential as a function of $n_{i\sigma}$.

Then, we use this analysis to introduce a DFT+U potential extending previous proposals to materials with arbitrarily high correlation. In particular, we find that this potential mainly screens the conventional mean field potential contribution, and also yields new terms associated with the number of atomic electrons. Our results show that the atomic correlation effects enhance the role played by the intra-atomic exchange interaction and favor the formation of magnetic solutions.

I. INTRODUCTION

Density Functional Theory (DFT) [1, 2] pervades the theoretical studies of condensed matter [3, 4] and chemical systems [5]. It is well-accepted that the Local Density Approximation (LDA) and related Generalized Gradient Approximations (GGAs) yield accurate results for systems not having important electron correlation effects. In LDA, following the Kohn-Sham approach [2], a local exchange-correlation potential for the electrons, $V_{xc}(\vec{r})$, is introduced as a function of the local charge density, $n(\vec{r})$; conventionally, this potential is calculated from the properties of the jellium model having a density n equal to the corresponding local charge $n(\vec{r})$. In GGA methods [6] this potential also depends on the local gradient of the electron density, $|\vec{\nabla}n(\vec{r})|$.

These approximations, however, do not describe properly some important properties for highly correlated systems such as the electronic density of states (DOS) (*e.g.* the position of the d or f bands (levels) in solids (molecules) containing transition metal atoms), or the correct (spin) ground state for different molecules and materials containing d or f elements, etc.

In order to properly describe those systems different many-body schemes have been developed, based mainly on a GW-approach [7, 8] and/or a Dynamical Mean Field (DMF) approximation [9]. A very successful alternative is the so called DFT+U method [10–14], much easier to manage computationally speaking and frequently used in the computational scientific community to explore the properties of highly correlated materials beyond the limitations of DFT calculations, see *e.g.* [15–30].

In the conventional DFT+U method a local orbital potential is introduced in the d or f orbitals of the material, associated with the Hubbard Hamiltonian of the localized electrons. This local orbital approach is closely related to an extension of the conventional DFT formalism [31, 32] whereby, using a local orbital basis set ϕ_μ , the total energy of the system can be written as a function of the orbital occupation numbers n_μ of the orbitals ϕ_μ . As discussed in section III, Hohenberg-Kohn theorems [1] and Kohn-Sham approach [2] can be applied to this case so that a local exchange-correlation potential, $V_{xc,\mu}$, can be associated with each (spin)-orbital of the basis set. This provides a way of obtaining a "local density" solution (working all the time in the local orbital basis) introducing self-consistency in the orbital occupation numbers, n_μ , without resorting to a $n(\vec{r})$ and $V(\vec{r})$ description. In

this approach, the atomic Hubbard model plays a similar role as the jellium model does for standard LDA or GGA methods.

The purpose of this paper is to analyze, going beyond the mean-field solution used in the conventional DFT+U approach, and within the local orbital formalism [31, 32] just mentioned, the many-body energy of a transition metal atom as described by the Kanamori Hamiltonian [33–35] (an extension of the atomic Hubbard one), assuming that the atom is embedded within an environment described by a set of channels, as shown in Figure 1. Using this Hubbard-Kanamori model we can analyze in detail its correlation energy, and discuss the effect of not only U , but also of the exchange interaction, J , in the many-body properties of the transition metal atom.

We notice that although in many applications a simplified version of the DFT+U technique has been used, whereby only a Hubbard U correction is considered, many authors have also analyzed a more general DFT+U approach where both the direct (Hubbard) U and the intra-atomic exchange (Hund’s rule coupling) J interactions are explicitly included, see, for example, references [13, 20, 25, 28, 36–38].

Our results for the Hubbard-Kanamori model are thus used to derive appropriate corrections, including electron correlation effects, to this more general DFT+U(+J) approach.

We should also mention that the solution presented here for an isolated magnetic atom could be extended to a more general case of many atoms by means of a DMF-approach [9, 39], by including in the environment the consistent potential of the other magnetic atoms.

In the present work, the correlation energy and the corresponding potential are analyzed in a first step for the simpler Hubbard case, allowing us to introduce some of the ideas that will be used further in our general analysis. Then, we proceed to analyze the Kanamori Hamiltonian and obtain a general expression for the correlation potential in terms of $n_{i\sigma}$ and the total number of electrons in the atom, \mathcal{N} . Finally, this result is used to define a DFT+U potential for a magnetic atom that includes correlation effects usually neglected in a mean field approximation [11, 40]. Our results show that correlation effects introduce an important screening in the conventional mean-field contribution to that DFT+U potential, and yield new terms associated with the one-electron levels of the magnetic atom.

II. THE ATOMIC HAMILTONIAN AND THE MODEL

We start by writing down the Kanamori-like Hamiltonian [33] for the $i\sigma$ -states of a magnetic atom with $2M$ -levels:

$$\begin{aligned} \hat{H}^A = & \sum_{i\sigma} \epsilon_{i\sigma} \hat{n}_{i\sigma} + U \sum_i \hat{n}_{i\uparrow} \hat{n}_{i\downarrow} + \frac{U'}{2} \sum_{i \neq j, \sigma} \hat{n}_{i\sigma} \hat{n}_{j\bar{\sigma}} + \\ & \frac{U' - J}{2} \sum_{i \neq j, \sigma} \hat{n}_{i\sigma} \hat{n}_{j\sigma} - \frac{J}{2} \sum_{i \neq j, \sigma} \hat{c}_{j\sigma}^\dagger \hat{c}_{j\bar{\sigma}} \hat{c}_{i\bar{\sigma}}^\dagger \hat{c}_{i\sigma} . \end{aligned} \quad (1)$$

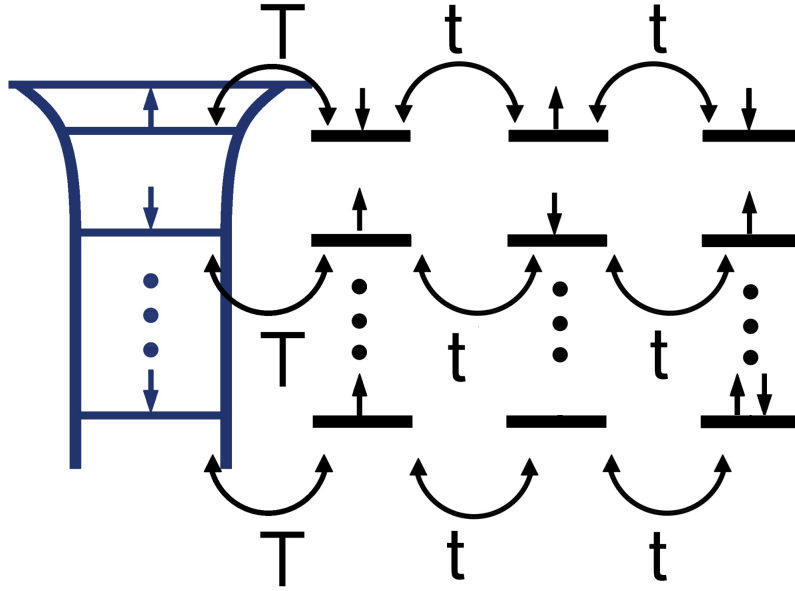


FIG. 1: (Color online) Schematic representation of our model system. An atomic shell of $2M$ $i\sigma$ -orbitals (left), described by the atomic Hamiltonian \hat{H}^{at} , eq. 1, is connected to different channels (right), that simulate the effect of the environment, by means of a one-electron Hamiltonian \hat{H}^{OE} , eq. 3. In our calculations, each channel is simulated by a chain of three sites; in each super-chain (the atomic level plus the chain) we assume to have always four electrons.

In Equation (1), $\hat{c}_{i\sigma}^\dagger$, $\hat{c}_{i\sigma}$ and $\hat{n}_{i\sigma}$ are the usual creation, annihilation and number operators, respectively, associated with the orbital (M) and spin (2) states ($i\sigma$). U (U') is the Coulomb-interaction between the $i\uparrow$, $i\downarrow$ ($i\uparrow$, $j\downarrow$) orbitals, while $U' - J$ is the interaction between $i\sigma$ and $j\sigma$. J represents the exchange interaction between orbitals with the same spin. The last term of Hamiltonian (1) represents a typical spin flip term for the $i\sigma$ and $j\sigma$ states, and its contribution is needed in order for the Hamiltonian to be rotationally invariant if

$U = U' + J$ [34]. In the Hubbard case, $J = 0$, $U = U'$ and \hat{H}^A is rotational invariant; this is very easy to see since, in this case, the atomic hamiltonian $\hat{H}^A = \frac{U}{2} \sum_{i,\sigma \neq j,\sigma'} \hat{n}_{i\sigma} \hat{n}_{j\sigma'}$ can be recasted as:

$$\hat{H}^A = \frac{U}{2} \hat{N} (\hat{N} - 1),$$

where \hat{N} is the total number of electrons operator, $\hat{N} = \sum_{i,\sigma} \hat{n}_{i\sigma}$. In the Hubbard-Hund case ($J > 0$), rotational symmetry is more involved, and, as commented above, depends on the particular relation between the many-body parameters. In this case, it is convenient to include also the total spin operator, $\hat{S} = \sum_{i,\sigma,\sigma'} \hat{c}_{i\sigma}^\dagger \vec{S}_{\sigma\sigma'} \hat{c}_{i\sigma'}$, where the $\vec{S}_{\sigma\sigma'}$ are Pauli's matrices.

For any number of orbitals, imposing the relationship $U = U' + J$ makes possible to recast our hamiltonian (1) as [34]:

$$\hat{H}^A = \left(U - \frac{3J}{2} \right) \frac{\hat{N} (\hat{N} - 1)}{2} - J \hat{S}^2, \quad (2)$$

as may be checked by a direct computation, expanding the operators. This makes explicit the rotational symmetry, since $[\hat{L}_i, \hat{S}^2] = 0$ and $[\hat{L}_i, \hat{N}] = 0$ for any component (i) of the angular momentum operator. For systems with three orbitals, if we add the double-hopping term to the atomic hamiltonian, $\frac{J}{2} \sum_{i \neq j, \sigma} \hat{c}_{i\sigma}^\dagger \hat{c}_{i\bar{\sigma}}^\dagger \hat{c}_{j\bar{\sigma}} \hat{c}_{j\sigma}$, the relationship, $U = U' + 2J$, which arises in a natural way when considering rotations of the p -orbitals, also takes us to a rotationally symmetric hamiltonian,

$$\hat{H}^A = (U - 3J) \frac{\hat{N} (\hat{N} - 1)}{2} - 2J \hat{S}^2 - \frac{J}{2} \hat{L}^2 + \frac{5}{2} J \hat{N},$$

which now includes an explicit dependence on the total angular momentum, whose components, in this case (three atomic orbitals), have the simple form $L_i = \sum_{ijk} \epsilon_{ijk} \hat{c}_{j\sigma}^\dagger \hat{c}_{k\sigma}$, where ϵ_{ijk} is the Levi-Civita symbol [34].

The atom described by the Kanamori Hamiltonian, equation (1), is embedded within a material. In our model, we assume each atomic orbital to interact with the environment through a channel that we simulate ideally by a semi-infinite 1-dimensional chain (Figure 1), using the following one-electron Hamiltonian:

$$\hat{H}^{\text{OE}} = \sum_{j\alpha\sigma} \epsilon_{j\alpha\sigma} \hat{n}_{j\alpha\sigma} + \sum_{j,\alpha \neq \beta, \sigma}^{n.n.} t \left(\hat{c}_{j\alpha\sigma}^\dagger \hat{c}_{j\beta\sigma} + \hat{c}_{j\beta\sigma}^\dagger \hat{c}_{j\alpha\sigma} \right) + \sum_{j\sigma} T \left(\hat{c}_{j\sigma}^\dagger \hat{c}_{j\alpha_1\sigma} + \hat{c}_{j\alpha_1\sigma}^\dagger \hat{c}_{j\sigma} \right), \quad (3)$$

where greek indexes (α, β) refer to states of one chain and j refers to the super-chain $\{j, j\alpha_1, \dots\}$.

It is interesting to realize that for $\epsilon_{j\sigma} = \epsilon_{j\alpha\sigma}$ and $t = T$ the one-electron DOS associated with \hat{H}^{OE} for the atomic orbital j (at the end of the semi-infinite 1-D superchain) is $\rho(E) = \frac{1}{\pi T} \sqrt{1 - (E/T)^2}$, for $-2T < E < 2T$; this suggests that for a given one-electron bandwidth, W , one should take $T \simeq W/4$ in our model. A more detailed argument [41] yields $T = W/\sqrt{12}$.

Calculating numerically the ground state of the many-body problem defined by the atom connected to several half-filled semi-infinite 1-D chains, $\hat{H}^t = \hat{H}^A + \hat{H}^{\text{OE}}$, is a formidable task. Thus, we take in each 1-D chain only three levels, a simplification that allows us to solve the many-body problem by exact diagonalization. In our calculations, we consider the space of electronic configurations defined by the conditions of having zero total spin and 4 electrons in each super-chain, as well as all the possible configurations obtained applying \hat{H}^t to that set of initial configurations. In particular, notice that due to the spin flip term in \hat{H}^A , the spin in each super-chain for a particular electronic configuration of the ground state of \hat{H}^t can be different from zero.

The value of t has been changed in a range from 0 to T , for $M = 2$ with only minor changes in the correlation energy and potential, see figures 9 and 15. This means that the fluctuations of charge in the atomic levels are mainly controlled by T , the hopping between the atomic orbitals and the first atomic level of each chain.

Accordingly, we have analyzed the cases $M = 3$ or $M = 5$ taking $t = 0$, *i.e.* reducing each chain to only one atom, since for $t \neq 0$ these calculations are numerically very demanding.

III. DFT FORMALISM FOR THE MANY-BODY HAMILTONIAN

Following the discussion of Refs. [31, 32, 42] we can adapt the Hohenberg-Kohn theory and Kohn-Sham approach to our formalism in terms of the orbital occupation numbers $\{n_\alpha\}$ corresponding to the local orbital basis set ϕ_α .

Hohenberg-Kohn theorems. (1) The set of occupation numbers $\{n_\alpha\}$ determines the external potentials $\{v_\alpha\}$ up to a constant.

Proof. Let us define two hamiltonians, $\hat{H}_v = \hat{H}_0 + \sum_\alpha v_\alpha \hat{n}_\alpha$ and $\hat{H}_u = \hat{H}_0 + \sum_\alpha u_\alpha \hat{n}_\alpha$. First, let us notice that, if $\{v_\alpha\}$ and $\{u_\alpha\}$ differ in more than a constant, the ground states $|\Phi_v\rangle$

and $|\Phi_u\rangle$ cannot be equal. To prove it, assume the opposite, so that we have $\hat{H}_v|\Phi\rangle = E_v|\Phi\rangle$ and $\hat{H}_u|\Phi\rangle = E_u|\Phi\rangle$. Subtracting both equations we get:

$$\sum_{\alpha} (v_{\alpha} - u_{\alpha}) \hat{n}_{\alpha} |\Phi\rangle = (E_v - E_u) |\Phi\rangle. \quad (4)$$

Calling $N = \langle \Phi | \hat{N} | \Phi \rangle$, the total number of electrons, consider next a basis set of Slater determinants $|\vec{\alpha}\rangle$, where the vector $\vec{\alpha} = (\alpha_1, \dots, \alpha_N)$ indicates the set of orbitals of our local basis set that define each $|\vec{\alpha}\rangle$ i.e., $|\vec{\alpha}\rangle$ is the Slater determinant formed by the $\phi_{\alpha_1}, \dots, \phi_{\alpha_N}$. Now, projecting eq. (4) over state $|\vec{\alpha}\rangle$ yields:

$$\sum_j (v_{\alpha_j} - u_{\alpha_j}) = (E_v - E_u) \quad (5)$$

for each $\vec{\alpha}$. In particular, given any α and any β , write down eq. (5) for $(\alpha, \alpha_2, \dots, \alpha_N)$ and $(\beta, \alpha_2, \dots, \alpha_N)$. Since $E_v - E_u$ is a constant, by subtracting the two equations we get that for all α and all β , it holds that $v_{\alpha} - u_{\alpha} = v_{\beta} - u_{\beta}$, which proves that indeed $|\Phi_v\rangle$ and $|\Phi_u\rangle$ cannot be equal if $\{v_{\alpha}\}$ and $\{u_{\alpha}\}$ differ in more than a constant.

Now the proof follows the same step as in the original proof by Hohenberg and Kohn: Assume the two hamiltonians \hat{H}_v and \hat{H}_u differing in more than a constant have the same occupation numbers $\{n_{\alpha}\}$. Then we can write

$$\begin{aligned} E_v &= \langle \Phi_v | \hat{H}_0 + \sum_{\alpha} v_{\alpha} \hat{n}_{\alpha} | \Phi_v \rangle < \langle \Phi_u | \hat{H}_0 + \sum_{\alpha} v_{\alpha} \hat{n}_{\alpha} | \Phi_u \rangle < \\ E_u &+ \langle \Phi_u | \sum_{\alpha} (v_{\alpha} - u_{\alpha}) \hat{n}_{\alpha} | \Phi_u \rangle = E_u + \sum_{\alpha} (v_{\alpha} - u_{\alpha}) n_{\alpha}. \end{aligned}$$

A similar argument interchanging the labels u and v , leads to the inequality $E_u < E_v + \sum_{\alpha} (u_{\alpha} - v_{\alpha}) n_{\alpha}$. Adding both inequalities we get the contradiction $E_v + E_u < E_u + E_v$, which proves the theorem.

In similarity to standard Hohenberg-Kohn theory, it follows that (2) the energy can be defined as a *function* of the occupation numbers, $E[\{n_{\alpha}\}]$, with the property

$$E[\{n_{\alpha}\}] \geq E[\{n_{\alpha}^0\}] = E_0, \quad (6)$$

where $\{n_{\alpha}^0\}$ is the set of ground state occupation numbers and E_0 the ground state energy. \square

Next, a **Kohn-Sham-like approach** can also be introduced.

Proof. Consider the general Hamiltonian

$$\hat{H} = \sum_{\alpha,\beta} \hat{c}_{\alpha}^{\dagger} \hat{c}_{\beta} \tau_{\alpha\beta} + \sum_{\alpha} v_{\alpha} \hat{n}_{\alpha} + \hat{U}_{ee} ,$$

where \hat{U}_{ee} is the electron-electron interaction (the many-body part of \hat{H}). First, we write the energy for \hat{H} as a function of the occupation numbers in the following way:

$$E[\{n_{\alpha}\}] = T_1[\{n_{\alpha}\}] + \sum_{\alpha} v_{\alpha} n_{\alpha} + E_H[\{n_{\alpha}\}] + E_{xc}[\{n_{\alpha}\}] ,$$

where E_H and E_{xc} are the Hartree and exchange-correlation energies; T_1 is defined using a system of non-interacting electrons,

$$\hat{H}_1 = \sum_{\alpha,\beta} \hat{c}_{\alpha}^{\dagger} \hat{c}_{\beta} \tau_{\alpha\beta} + \sum_{\alpha} v_{\alpha}^1 \hat{n}_{\alpha}$$

where the potentials $\{v_{\alpha}^1\}$ are chosen so that the solution of \hat{H}_1 yields, precisely, the occupation numbers $\{n_{\alpha}\}$. Then,

$$T_1[\{n_{\alpha}\}] = E_1[\{n_{\alpha}\}] - \sum_{\alpha} v_{\alpha}^1 n_{\alpha} ,$$

where $E_1[\{n_{\alpha}\}]$ is the ground state energy for \hat{H}_1 . Now, the ground state occupation numbers can be obtained considering the variational principle, eq. (6), which yields:

$$\sum_{\alpha} \delta n_{\alpha} \left[\frac{\partial T_1}{\partial n_{\alpha}} + v_{\alpha} + \frac{\partial E_H}{\partial n_{\alpha}} + \frac{\partial E_{xc}}{\partial n_{\alpha}} \right] = 0$$

(subject to the constrain of conservation of the total number of electrons, $\sum_{\alpha} \delta n_{\alpha} = 0$).

Applying the same argument for $E_1[\{n_{\alpha}\}]$ yields

$$\sum_{\alpha} \delta n_{\alpha} \left[\frac{\partial T_1}{\partial n_{\alpha}} + v_{\alpha}^1 \right] = 0 ;$$

these results show that the ground state occupation numbers $\{n_{\alpha}\}$ can be obtained by solving the one-particle Hamiltonian \hat{H}_1 , with the following "Kohn-Sham" potentials

$$v_{\alpha}^1 = v_{\alpha} + \frac{\partial E_H}{\partial n_{\alpha}} + \frac{\partial E_{xc}}{\partial n_{\alpha}} .$$

□

Coming back to our problem, $\hat{H}^t = \hat{H}^A + \hat{H}^{OE}$, equations (1) and (3), we can now apply these ideas and write the total energy, E^t , associated with \hat{H}^t as

$$E^t[\{n_{i\sigma}\}] = E^{\text{OE}} + E^A = E^{\text{OE}} + \sum_{i\sigma} \epsilon_{i\sigma} n_{i\sigma} + E_H^A[\{n_{i\sigma}\}] + E_{\text{corr}}^A[\{n_{i\sigma}\}] , \quad (7)$$

where $E^{\text{OE}} = \langle \hat{H}^{\text{OE}} \rangle$, E_H^A and E_{corr}^A being the Hartree and correlation energies of \hat{H}^A (in this model the atomic $\langle \hat{c}_{i\sigma}^\dagger \hat{c}_{j\sigma'} \rangle = 0$ so that the atomic exchange energy is zero; for a discussion on how to include atomic exchange effects, see ref. [32]). These quantities, E^{OE} , E_H^A and E_{corr}^A , can be calculated using the Kohn-Sham approach and the exact solution of the effective Hamiltonian:

$$\hat{H}^{\text{eff}} = \hat{H}^{\text{OE}} + \sum_{i\sigma} \epsilon_{i\sigma} \hat{n}_{i\sigma} + \sum_{i\sigma} (V_{H,i\sigma}^A + V_{\text{corr},i\sigma}^A) \hat{n}_{i\sigma}$$

where $V_{H,i\sigma}^A = \partial E_H^A / \partial n_{i\sigma}$ and $V_{\text{corr},i\sigma}^A = \partial E_{\text{corr}}^A / \partial n_{i\sigma}$. The Hartree energy is computed by applying the mean-field approximation for all the many-body elements in hamiltonian (1) and neglecting off-diagonal terms, which are zero in this model:

$$\begin{aligned} E_H^A[\{n_{i\sigma}\}] &= U \sum_i n_{i\uparrow} n_{i\downarrow} + \frac{U'}{2} \sum_{i \neq j} n_{i\sigma} n_{j\bar{\sigma}} + \frac{U' - J}{2} \sum_{i \neq j} n_{i\sigma} n_{j\sigma} = \\ &= \frac{U' - J}{2} \mathcal{N}(\mathcal{N} - 1) + \frac{U' - J}{2} \sum_{i\sigma} n_{i\sigma} (1 - n_{i\sigma}) + J \mathcal{N}_\uparrow \mathcal{N}_\downarrow + J \sum_i n_{i\uparrow} n_{i\downarrow} , \end{aligned} \quad (8)$$

where $\mathcal{N}_\sigma = \sum_i n_{i\sigma}$ and $\mathcal{N} = \mathcal{N}_\uparrow + \mathcal{N}_\downarrow$. It is also convenient to present here the Hartree potential:

$$V_{H,i\sigma}^A = (U' - J)(\mathcal{N} - \frac{1}{2}) + (U' - J)(\frac{1}{2} - n_{i\sigma}) + J(\mathcal{N}_{\bar{\sigma}} + n_{i\bar{\sigma}}).$$

Let us now calculate the exact atomic energy, E^A , in the limit $U/T \rightarrow \infty$ (which was calculated for the Hubbard case ($J = 0$) in [12]) taking into account the first Hund-rule. For ease of notation, let us now omit the trivial one-electron part, $\sum_{i\sigma} \epsilon_{i\sigma} \hat{n}_{i\sigma}$, and write only the many-body part. To that end, we first calculate the energy for the case of an integer number, N , of electrons in the atom. Letting Θ denote the Heaviside step function and M the number of i -orbitals, we have, for the atomic limit and the Hund regime:

$$E^A(N) = (U' - J) \frac{N(N - 1)}{2} + J(M + 1)(N - M)\Theta(N - M)$$

The first term, which is the result when the atom is no more than half-filled (*i.e.* $N \leq M$), follows from the fact that, according to the first of Hund's rules, all electrons must have a parallel spin. If there is a number of electrons N (with $N \leq M$), each pair of electrons adds an energy $U' - J$ to the system and there is a total of $\frac{N(N - 1)}{2}$ pairs, hence the result.

For the case of the atom with $N > M$, an analogous reasoning can be made with the holes instead of the electrons, and the second term in the equation above is just the additional energy of the system, again directly computable from the hamiltonian in eq. (1).

When the average charge is a general \mathcal{N} , the system will fluctuate between the eigenstates with N and $N + 1$ electrons, $N < \mathcal{N} < N + 1$, where N is an integer number. Each of these states has a weight, respectively, α and β which must satisfy $\alpha + \beta = 1$, but also $N\alpha + (N + 1)\beta = \mathcal{N}$. From these two relations we have: $\alpha = N - \mathcal{N} + 1$ and $\beta = \mathcal{N} - N$, and then we finally obtain

$$E^A = (N - \mathcal{N} + 1) E^A(N) + (\mathcal{N} - N) E^A(N + 1) = \frac{U' - J}{2} N (2\mathcal{N} - N - 1) + J(M + 1)(\mathcal{N} - M)\Theta(\mathcal{N} - M), \quad (9)$$

where strictly $\sum_{i\sigma} \varepsilon_{i\sigma} n_{i\sigma}$ should be added. Combining Equations (8) and (9) leads to the following correlation energy (see equation 7):

$$E_{corr}^A[\{n_{i\sigma}\}] = E^A - E_H^A - \sum_{i\sigma} \varepsilon_{i\sigma} n_{i\sigma} = \frac{U' - J}{2} \delta\mathcal{N}(1 - \delta\mathcal{N}) - \frac{U' - J}{2} \sum_{i\sigma} n_{i\sigma}(1 - n_{i\sigma}) + J(M + 1)(\mathcal{N} - M)\Theta(\mathcal{N} - M) - J\mathcal{N}_{\uparrow}\mathcal{N}_{\downarrow} - J \sum_i n_{i\uparrow} n_{i\downarrow}, \quad (10)$$

for $U/T \rightarrow \infty$, where $\delta\mathcal{N} = \mathcal{N} - N$ takes values between 0 and 1, $0 < \delta\mathcal{N} < 1$.

For U/T finite we do not have an analytic solution; in this general case we proceed as follows:

(1) Calculate the ground state of $\hat{H}^t = \hat{H}^A + \hat{H}^{OE}$ (by exact diagonalization) for different values of U/T ; this yields the energy E^t and the occupation numbers $\{n_{i\sigma}\}$. Also, the Hartree energy can be calculated using eq. (8).

(2) Obtain the effective potentials, $V_{eff,i\sigma}^A = V_{H,i\sigma}^A + V_{corr,i\sigma}^A$, that reproduce the many-body occupation numbers, $\{n_{i\sigma}\}$. This yields the correlation potential, $V_{corr,i\sigma}^A$, as well as E^{OE} , E^A , and the correlation energy, E_{corr}^A .

In the following section we present the results that we obtain with this procedure. In a first step we analyze the simpler Hubbard case, and then we proceed to analyze the more general Hubbard-Hund case.

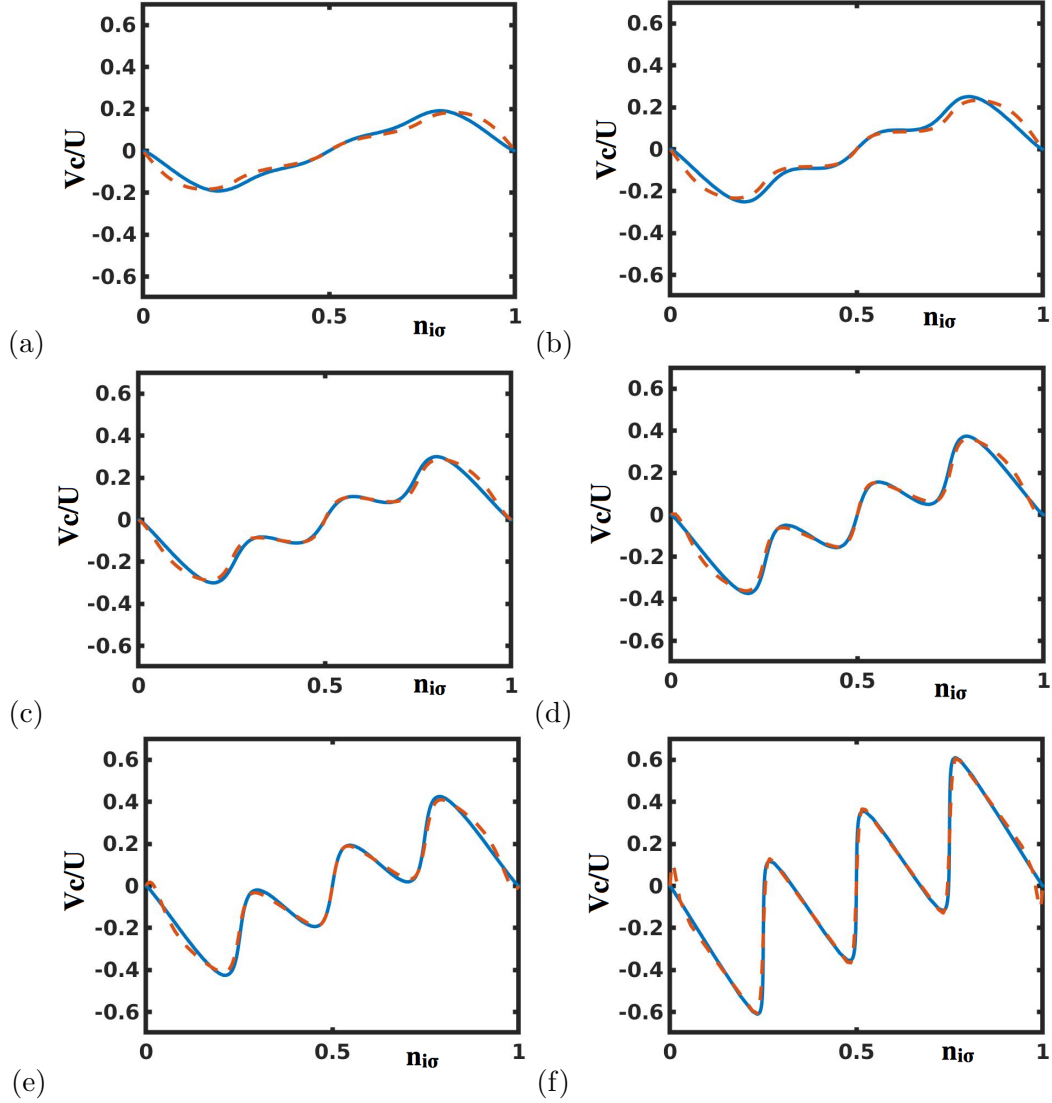


FIG. 2: (Color online) Correlation potential, $V_{corr,i\sigma}^A$, as a function of $n_{i\sigma}$ for $M = 2$ in units of U in the Hubbard case for $U/T = 4$ (a), 6 (b), 8 (c), 12 (d), 16 (e), 64 (f). Blue solid line: exact (numerical) correlation potential. Dashed orange line: fit using eqs. 12 and 13.

IV. RESULTS.

A. The Hubbard case

We present our results discussing first the case $\epsilon_{i\sigma} = 0$, $n_{i\sigma} = \mathcal{N}/2M$ and $M = 2$, in the Hubbard limit: $J=0$ and $U = U'$. Figure 2 shows V_{corr}^A for $U/T = 4, 6, 8, 12, 16, 64$ as a

function of $n_{i\sigma}$. For $U/T = 64$, the result is close to the atomic limit:

$$V_{corr,i\sigma}^A(n_{i\sigma}) = -U \left(\frac{1}{2} - n_{i\sigma} \right) + U \left(\frac{1}{2} - \delta\mathcal{N} \right), \quad (J = 0). \quad (11)$$

$U \left(\frac{1}{2} - \delta\mathcal{N} \right)$ is represented in Fig. 3a showing a periodic sawtooth behaviour, in correspondence with the atomic levels shown in Fig. 3b.

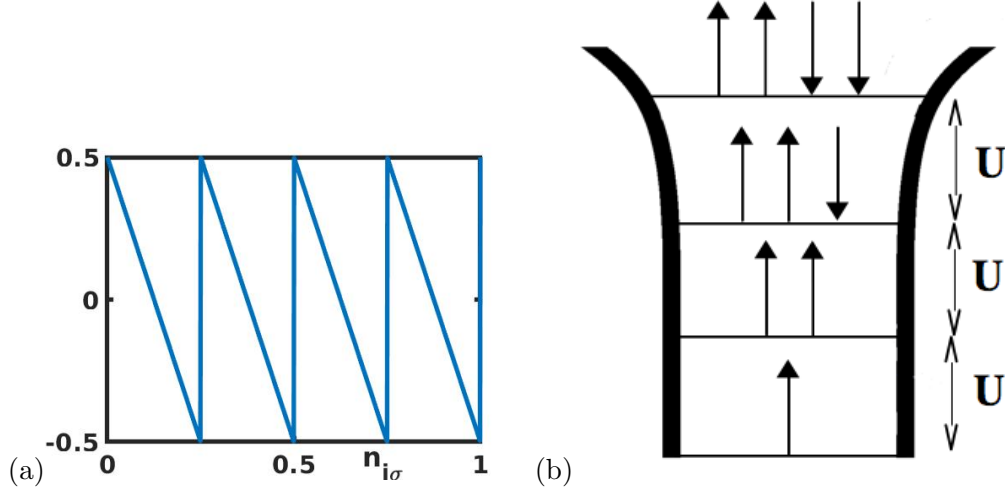


FIG. 3: (a) Sawtooth behaviour of the periodic part of the correlation potential, $U \left(\frac{1}{2} - \delta\mathcal{N} \right)$, in units of U for $M = 2$; $\mathcal{N} = \sum_{i\sigma} n_{i\sigma}$. The jump between the minima and the maxima is exactly U . (b) Atomic levels $E^A(N) - E^A(N-1) = 0, U, 2U, 3U$, for different atomic charges, $N = 1, 2, 3, 4$. Notice that the jump in the atomic levels corresponds to the jump in $U \left(\frac{1}{2} - \delta\mathcal{N} \right)$.

We can also write eq. (11) as $V_{corr,i\sigma}^A = U(-\delta\mathcal{N} + n_{i\sigma})$. Combining this with the Hartree potential, $V_{H,i\sigma}^A = U(\mathcal{N} - n_{i\sigma})$, this shows that $V_{eff,i\sigma}^A = V_{H,i\sigma}^A + V_{corr,i\sigma}^A = UN$, indicating that in this limit $V_{eff,i\sigma}^A$ is discontinuous, with the atomic level jumping by U when \mathcal{N} crosses an integer number. Equation (11) suggests to fit the calculated values of $V_{corr,i\sigma}^A$ for different values of U/T (see Figure 2) by means of the equation:

$$V_{corr,i\sigma}^A = -F_1 U \left(\frac{1}{2} - n_{i\sigma} \right) + F_2 U \left(\frac{1}{2} - \delta\mathcal{N} \right), \quad (J = 0); \quad (12)$$

where

$$F_k(x) = f_k \tanh(\alpha_k x(1-x)) \quad (13)$$

($k = 1, 2$), $x = n_{i\sigma}$ or $\delta\mathcal{N}$, and α_k is a constant. The tanh function has been chosen to describe a smooth matching for F_k between 0 and f_k with an effective width of α_k^{-1} .

U/T	4	6	8	12	16	32	64
f_1	(0.60) 0.58	(0.67) 0.62	(0.78) 0.68	(0.86) 0.71	(0.89) 0.71	(0.94) 0.80	(0.96) 0.89
f_2	(0.09) 0.15	(0.20) 0.24	(0.30) 0.31	(0.42) 0.49	(0.52) 0.60	(0.71) 0.82	(0.85) 0.92
f_3	0.15	0.24	0.35	0.51	0.65	0.79	1.0
α_1	(8.6) 9.1	(9.1) 10.2	(9.8) 12.2	(12.4) 19.6	(14.3) 20.1	(36.3) 51.1	(50.0) 52.3
α_2	(0.01) 0.08	(0.4) 0.8	(5.6) 6.2	(8.0) 8.2	(9.3) 14.1	(20.3) 17.5	(32.6) 32.1
α_3	25.2	41.2	48.7	63.4	78.5	87.3	165.5
α_4	17.0	20.8	31.0	33.1	38.0	51.4	196.1

TABLE I: Table I shows f_i and α_i for the Hubbard (in parenthesis) and Hubbard-Hund cases ($M = 2$).

In these Equations $F_1(n_{i\sigma}) \approx f_1$ (constant) and $F_2(\delta\mathcal{N}) \approx f_2$ (constant, too) except for $n_{i\sigma}$ or $\delta\mathcal{N}$, respectively, close to 0 and 1, since α_1 and α_2 in eq. (13) are typically much larger than 1;

Table I shows f_1 , f_2 , α_1 and α_2 for $U/T = 4, 6, 8, 12, 16$ and 64 . For $U/T \ll 4$, our fitting (not shown) yields $f_1 \approx f_2 \approx 0$ because in the small- U limit, E_{corr}^A and $V_{corr,i\sigma}^A$ go to zero as U^2/T , as indicated by second order perturbation theory; on the other hand, as mentioned above, for $U/T \geq 64$, the system is close to the atomic limit with f_1 and f_2 approaching 1. Equation (12) shows that in this Hubbard case $V_{corr,i\sigma}^A$ has two components; the first one, $-F_1U \left(\frac{1}{2} - n_{i\sigma} \right)$, tends to screen the Hartree component, $U \left(\frac{1}{2} - n_{i\sigma} \right)$, while the second one, $F_2U \left(\frac{1}{2} - \delta\mathcal{N} \right)$, reflects the influence of the atomic levels in the correlation potential. The effect of this second component is well appreciated in the oscillating behaviour of $V_{corr,i\sigma}^A$ as shown in Figure 2: it is small for $U/T = 4$ or 6 , but increases to almost full value for $U/T = 64$.

Figure 4 shows $V_{eff,i\sigma}^A$ for different values of U/T . Notice that, in accordance with equation (12), the effective potential can be approximated by

$$V_{eff,i\sigma}^A \approx (1 - F_1)U \left(\frac{1}{2} - n_{i\sigma} \right) + U \left(\mathcal{N} - \frac{1}{2} \right) + F_2U \left(\frac{1}{2} - \delta\mathcal{N} \right); \quad (J = 0). \quad (14)$$

For $U/T = 64$, f_1 and f_2 approach 1, so that $V_{eff,i\sigma}^A$ is close to the atomic limit ($f_1 \approx f_2 \approx 1$) with a staircase behavior. For $U/T = 4$, $V_{eff,i\sigma}^A$ is close to a straight line, indicating

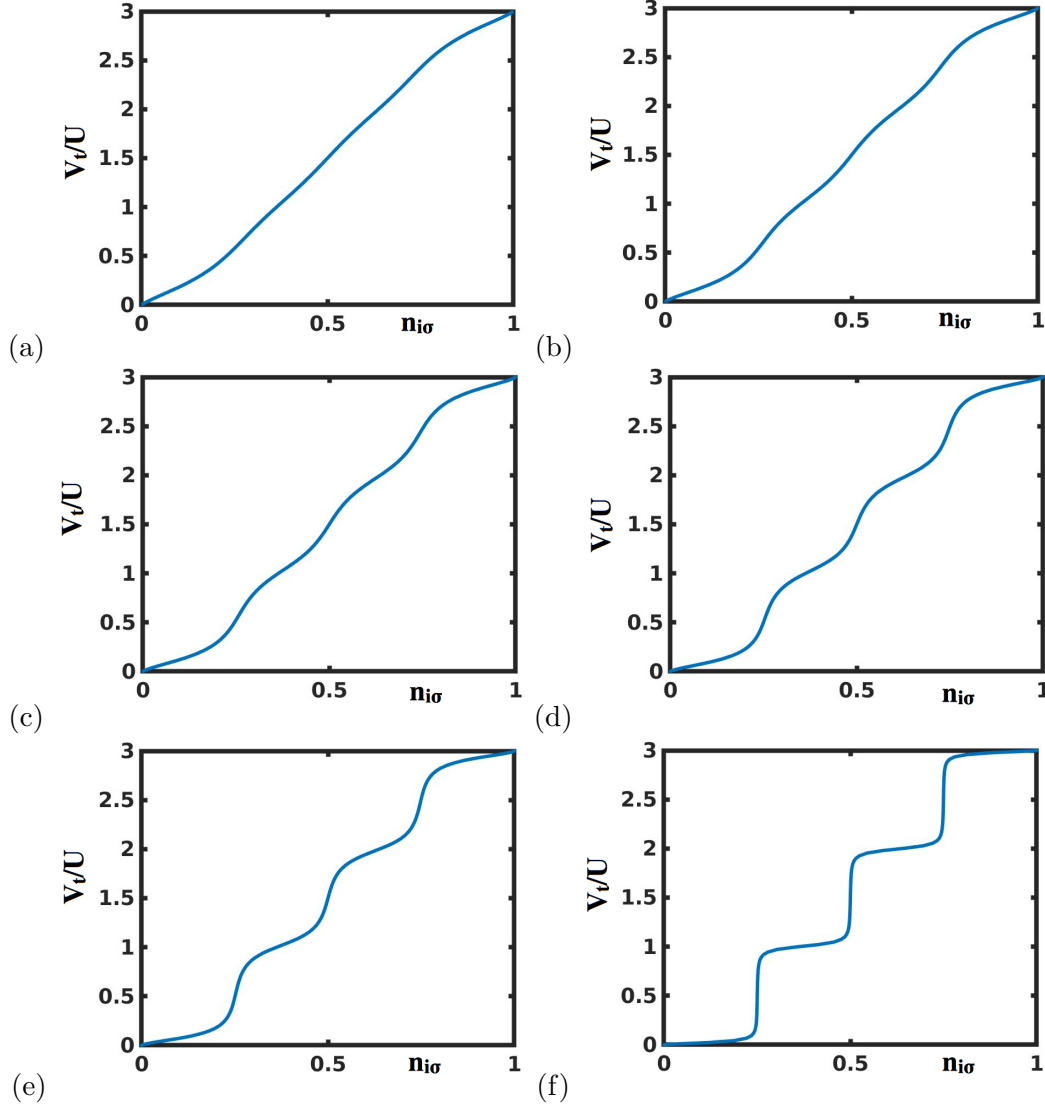


FIG. 4: Effective potential as a function of $n_{i\sigma}$ in units of U , $V_{eff,i\sigma}^A = V_{H,i\sigma}^A + V_{corr,i\sigma}^A$, in the Hubbard case for $U/T=4, 6, 8, 12, 16, 64$, ($M = 2$).

that we can neglect the fluctuating term $F_2 U (\frac{1}{2} - \delta\mathcal{N})$, and approximate Equation (14) by $(1 - F_1)U (\frac{1}{2} - n_{i\sigma}) + U (\mathcal{N} - \frac{1}{2})$, and $V_{corr,i\sigma}^A$ by $-F_1 U (\frac{1}{2} - n_{i\sigma})$.

Notice that equation (14) is valid in the limit $U/T \rightarrow 0$, $F_1 \approx F_2 \approx 0$, for any values of $n_{i\sigma}$ even if $n_{i\sigma} \neq n_{j\sigma'}$. Moreover, it should be also realized that the atomic limit, $U/T \rightarrow \infty$, of E^A in eq. (9) for $J = 0$, $\frac{1}{2}UN(2\mathcal{N} - N - 1)$, only depends on the energy of the states with N and $(N + 1)$ electrons, a value that is independent from the particular occupation of the $i\sigma$ states. This indicates that the atomic limit of eq. (14) is also valid for $n_{i\sigma} \neq n_{j\sigma'}$. Those two limits suggest that eq. (14) is an appropriate interpolation of $V_{eff,i\sigma}^A$ for $n_{i\sigma} \neq n_{j\sigma'}$ with

F_1 and F_2 close to the values given in Table I. This has been checked calculating the case $n_{1\uparrow} = n_{1\downarrow} \neq n_{2\uparrow} = n_{2\downarrow}$. Figure 5 shows $V_{corr,i\sigma}^A$ along the lines $n_{1\sigma} - n_{2\sigma} = 0.1$; $n_{1\sigma} + n_{2\sigma} = 1$ and $n_{1\sigma} + n_{2\sigma} = 0.9$ for $U/T = 12$, compared with eq. (12). For $n_{1\sigma} - n_{2\sigma} = 0.1$, V_{corr}^A is similar to the curve shown in Figure 2d, where $n_{1\sigma} - n_{2\sigma} = 0$. For cases b) and c) $n_{1\sigma} + n_{2\sigma}$ and the total charge, \mathcal{N} , and $\delta\mathcal{N}$ are constant; then, equation (12) shows that the correlation potential along the corresponding curves depends on $n_{1\sigma} - n_{2\sigma}$ (and changes linearly when $0 \ll n_{i\sigma} \ll 1$), as shown in Figure 5.

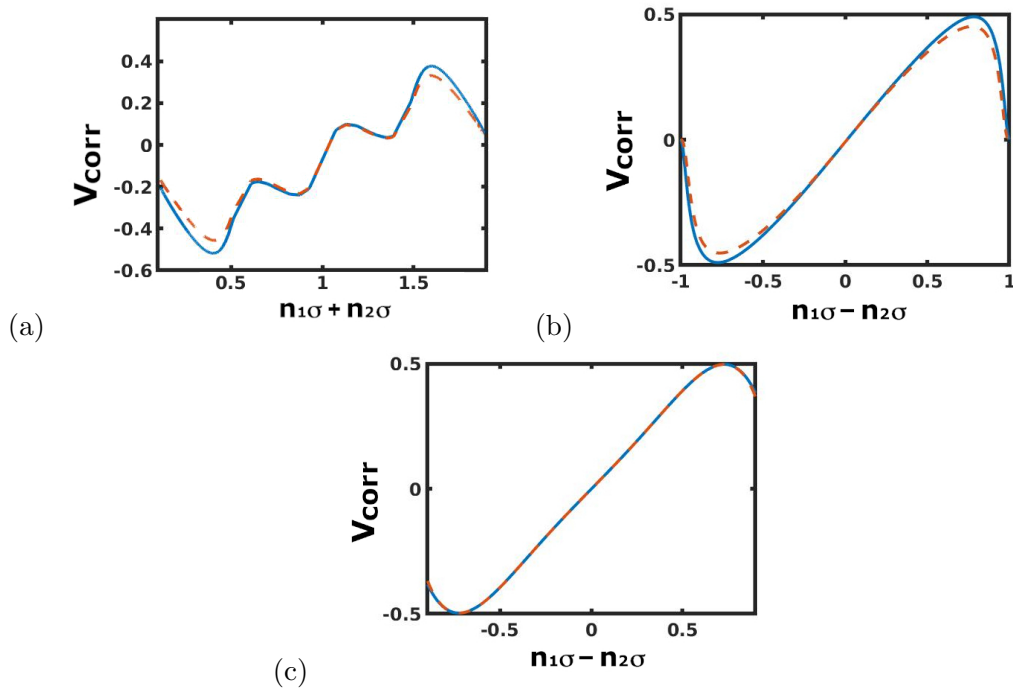


FIG. 5: (Color online) Correlation potential, $V_{corr,i\sigma}$, in units of U , in the Hubbard case for $U/T = 12$ along different relevant directions: (a) $n_{1\uparrow} - n_{2\uparrow} = 0.1$; (b) $n_{1\uparrow} + n_{2\uparrow} = 1$; (c) Curve $n_{1\uparrow} + n_{2\uparrow} = 0.9$. The potentials are calculated as derivatives of the correlation energy along the direction of the corresponding lines $n_1 \pm n_2 = \text{const}$; these potentials are plotted against $n_1 \mp n_2$. The solid blue line is the exact result, while the dashed line represents our fit using eqs. (12) and (13).

B. The Hubbard-Hund case.

Figure 6 shows our numerical results for $V_{corr,i\sigma}^A$ taking $J = 0.1U$ and $U = U' + J$. In the atomic limit, $U/T \rightarrow \infty$, $V_{corr,i\sigma}^A$ is given by (see eq. (10)):

$$V_{corr,i\sigma}^A = -(U' - J) \left(\frac{1}{2} - n_{i\sigma} \right) + (U' - J) \left(\frac{1}{2} - \delta\mathcal{N} \right) - J(\mathcal{N}_{\bar{\sigma}} + n_{i\bar{\sigma}}) + (M + 1)J\Theta(\mathcal{N} - M). \quad (15)$$

Notice that the first two terms of this equation coincide with Equation (11) changing U by $(U' - J)$; the last two terms are new contributions associated with J . Equation (15) suggests to fit our calculations for $V_{corr,i\sigma}^A$ (see Figure 6) by the following potential:

$$V_{corr,i\sigma}^A = -F_1(U' - J) \left(\frac{1}{2} - n_{i\sigma} \right) + F_2(U' - J) \left(\frac{1}{2} - \delta\mathcal{N} \right) - F_3J(\mathcal{N}_{\bar{\sigma}} + n_{i\bar{\sigma}}) + F_4J(M + 1) \quad (16)$$

where F_1 and F_2 have the same functional form as in equation (13), and:

$$F_3 = f_3 \tanh(\alpha_3 x (M + 1 - x)); \quad (x = \mathcal{N}_{\bar{\sigma}} + n_{i\bar{\sigma}}) \quad (17)$$

$$F_4 = f_3 / [1 + \exp(-\alpha_4(\mathcal{N} - M))]$$

As in the Hubbard case, we can write $F_1 \approx f_1$, $F_2 \approx f_2$ and $F_3 \approx f_3$ if the corresponding variables are not close to their edge limits: 0 or 1 for $n_{i\sigma}$ and $\delta\mathcal{N}$, 0 or $M + 1$ for $x = \mathcal{N}_{\bar{\sigma}} + n_{i\bar{\sigma}}$; also, $F_4 \rightarrow f_3\Theta(\mathcal{N} - M)$ if \mathcal{N} is not close to M . On the other hand, for small values of U/T ($U/T \ll 4$), $f_i \rightarrow 0$, and $V_{eff,i\sigma}^A = V_{H,i\sigma}^A$ is given by:

$$V_{eff,i\sigma}^A = (U' - J) \left(\frac{1}{2} - n_{i\sigma} \right) + (U' - J) \left(\mathcal{N} - \frac{1}{2} \right) + J(\mathcal{N}_{\bar{\sigma}} + n_{i\bar{\sigma}}), \quad (18)$$

while for U/T large ($U/T \gg 64$) $f_i \rightarrow 1$ and

$$V_{eff,i\sigma}^A = (U' - J) \left(\mathcal{N} - \frac{1}{2} \right) + (U' - J) \left(\frac{1}{2} - \delta\mathcal{N} \right) + J(M + 1)\Theta(\mathcal{N} - M). \quad (19)$$

The last two terms in this equation are associated with the jump in the energy levels of the isolated atom, see Figure 7. While $(U' - J) \left(\frac{1}{2} - \delta\mathcal{N} \right)$ yields the see-saw behaviour with $E(N + 1) - E(N) = U' - J$, for $N \neq M$, $J(M + 1)\Theta(\mathcal{N} - M)$ is associated with the energy difference $E(M + 1) - E(M) = U' + MJ$ between the M and $M + 1$ levels.

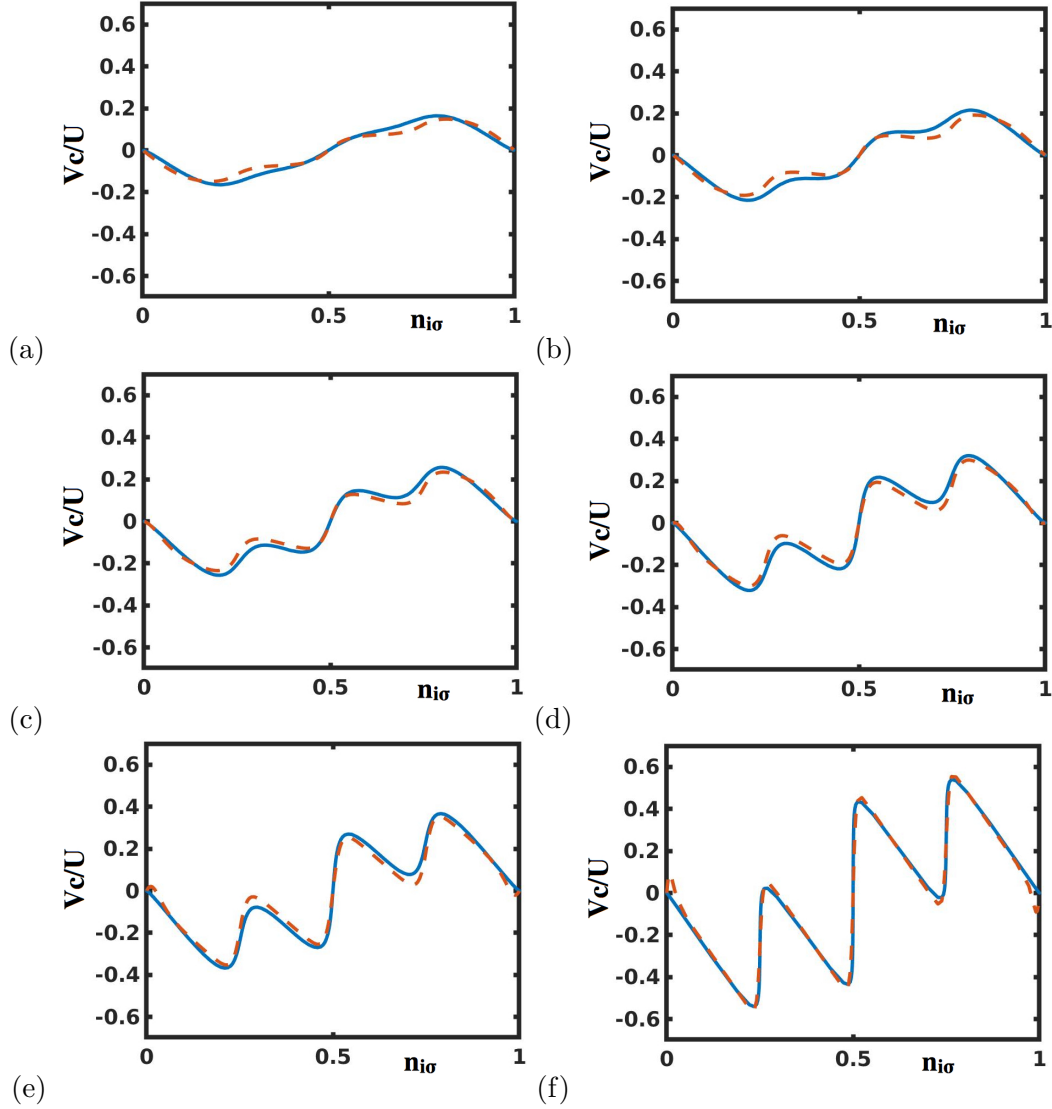


FIG. 6: (Color online) Correlation potential, $V_{corr,i\sigma}^A$, as a function of $n_{i\sigma}$ ($M = 2$) in units of U in the Hubbard-Hund case for $U/T=4, 6, 8, 12, 16, 64$. Blue solid line: exact (numerical) correlation potential. Dashed orange line: fit using eqs. 16, 13 and 17.

In general, from our fit for $V_{corr,i\sigma}^A$, we see that $V_{eff,i\sigma}^A$ (Figure 8) can be well-fitted by:

$$V_{eff,i\sigma}^A = (1 - F_1) (U' - J) \left(\frac{1}{2} - n_{i\sigma} \right) + (U' - J) \left(\mathcal{N} - \frac{1}{2} \right) + F_2 (U' - J) \left(\frac{1}{2} - \delta \mathcal{N} \right) + (1 - F_3) J (\mathcal{N}_{\bar{\sigma}} + n_{i\bar{\sigma}}) + F_4 J (M + 1). \quad (20)$$

We show in Table I the values of $f_1, f_2, f_3, \alpha_1, \alpha_2, \alpha_3, \alpha_4$ as calculated in our fitting. In general, f_1 and f_2 are similar to the values given for the Hubbard case, although f_1 is a little smaller (and f_2 a little larger): this is due to the effective U of this case that is smaller, $U' - J = U - 2J = 0.8U$. While in the Hubbard case f_1 varies monotonically, in

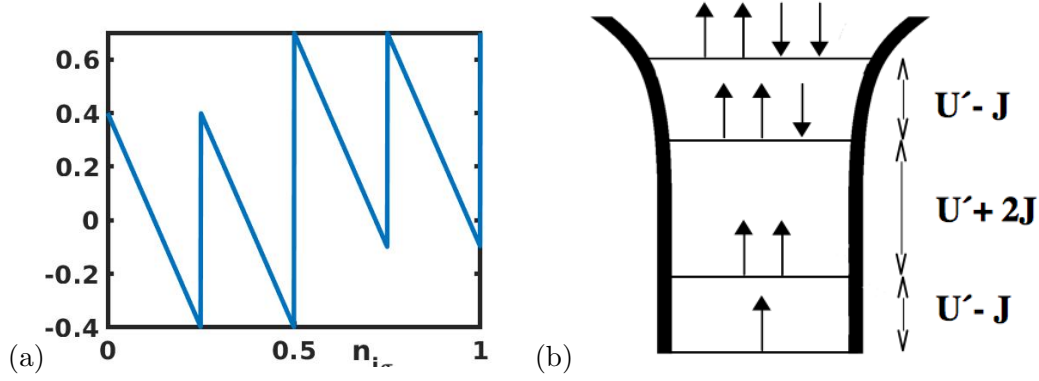


FIG. 7: (a) Sawtooth behaviour of $(U' - J) \left(\frac{1}{2} - \delta N\right) + J(M + 1)\Theta(N - M)$, see equations (15) and (19), in units of U for $M = 2$; (b) Atomic levels, $E^A(N) - E^A(N - 1) = 0$, $U' - J$, $2U' + J$, $3U'$, for different atomic charges, $N = 1, 2, 3, 4$. Compare with fig. 3; the jump between the levels for three and two electrons, $U' + 2J$ is reflected in the jump in (a) for $n_{i\sigma} = 0.5$.

the Hubbard-Hund case it is observed to have a plateau for values of U/T between 8 and 16. This seems to be due to the transition to the Hubbard-Hund regime: indeed, defining the Hund subspace as those configurations satisfying the first Hund rule, we have calculated that the projection of the ground state over the Hund subspace is 66 %, 83%, and 95% for $U/T = 4, 8$ and 12, respectively. It is also interesting to realize that for $U/T \leq 6$, f_2 and f_3 are small so that $V_{eff,i\sigma}^A$ can be approximated by

$$V_{eff,i\sigma}^A = (1 - F_1) (U' - J) \left(\frac{1}{2} - n_{i\sigma}\right) + (U' - J) \left(\mathcal{N} - \frac{1}{2}\right) + J (\mathcal{N}_{\bar{\sigma}} + n_{i\bar{\sigma}}). \quad (21)$$

In this case, only the term $(U' - J) \left(\frac{1}{2} - n_{i\sigma}\right)$ is screened to $(1 - F_1) (U' - J) \left(\frac{1}{2} - n_{i\sigma}\right)$ by correlation effects while the exchange contribution $J (\mathcal{N}_{\bar{\sigma}} + n_{i\bar{\sigma}})$ remains almost unchanged. Notice also that $(1 - f_1)$ decreases when $(U' - J)$ increases; these two effects partially compensate each other in the variation of the first term in eq. (21) as a function of U/T .

C. M=3 and M=5.

Up to now, we have considered $M=2$ with 3 levels ($m=3$) in each of the two channels introduced in our model, see Figure 1. Analyzing a similar case with $M= 3$ or 5 is not an easy task because the exact solution of the corresponding many-body problem is numerically very demanding. Then, we have taken for $M = 3$ or 5, channels with only one level ($m =$

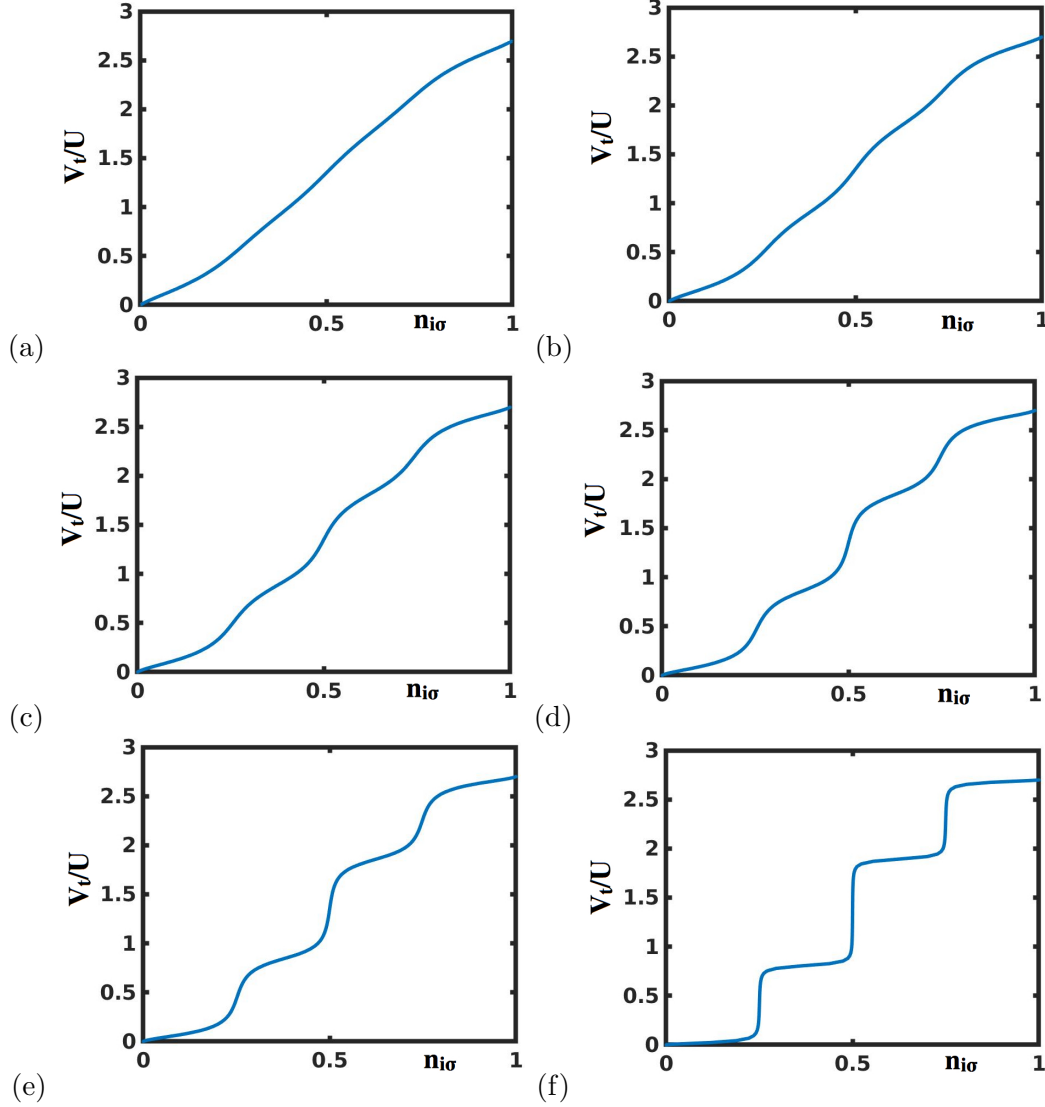


FIG. 8: Effective potential, $V_{eff,i\sigma}^A = V_{H,i\sigma}^A + V_{corr,i\sigma}^A$, as a function of $n_{i\sigma}$ in units of U , in the Hubbard-Hund case for $U/T=4, 6, 8, 12, 16, 64$.

1); this simplification yields a good approximation to the more complete case with $m = 3$ as we have checked analyzing both cases for $M = 2$. Thus, Figure 9 shows $V_{corr,i\sigma}^A$ for the Hubbard-Hund case, $M = 2$ and $m = 1$ or 3 ; the values taken for U/T are the same as in the other figures. We have calculated the case $m = 3$ for different values of t , the hopping between the levels on the chain. We find that the deviation from the case $t = 0$ (which corresponds to $m = 1$) is monotonously increasing and very small ($\leq 5\%$) for any value of t between 0 and $2T$. The comparison of both cases shows that $V_{corr,i\sigma}^A$ is only slightly changed between $m = 1$ or 3 .

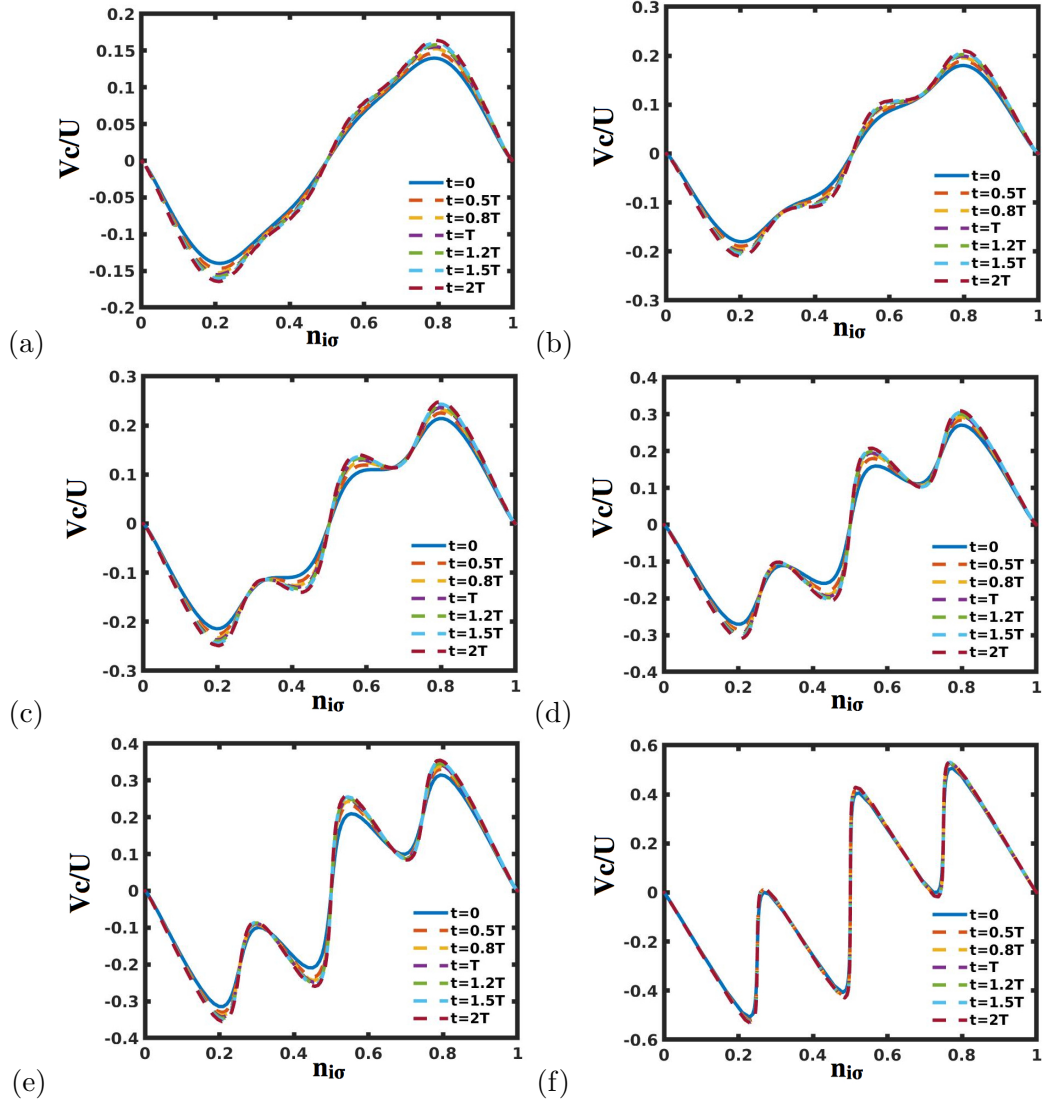


FIG. 9: Correlation potential as a function of $n_{i\sigma}$ in units of U in the Hubbard-Hund case for different values of t between 0 and $2T$, for $U/T = 4, 6, 8, 12, 16, 64$, and $M = 2$, $m = 3$. The solid blue line ($t = 0$) corresponds to the $M = 2, m = 1$ case.

Figure 10 shows $V_{corr,i\sigma}^A$ for $M = 3$ and $m = 1$, Figure 11 shows the result for $M = 5$ and $m = 1$, in both cases for the Hubbard-Hund case. Tables II and III give the values of $f_1, f_2, f_3, \alpha_1, \alpha_2, \alpha_3$ and α_4 for $M = 3$ or 5 , and $m = 1$, as calculated in our best fitting to $V_{corr,i\sigma}^A$, as given by equation (16).

As in the case $M = 2$, for $U/T \leq 6$, $V_{eff,i\sigma}^A$ can also be approximated by eq. (21), with the term $(U' - J)(1/2 - n_{i\sigma})$ screened to $(1 - F_1)(U' - J)(1/2 - n_{i\sigma})$ and the exchange contribution, $J(\mathcal{N}_{\bar{\sigma}} + n_{i\bar{\sigma}})$ unchanged (see Appendix A.2).

It is interesting to mention that in the more general Kanamori Hamiltonian, where the double hopping term, $\frac{J}{2} \sum_{i \neq j} \hat{c}_{i\sigma}^\dagger \hat{c}_{i\bar{\sigma}}^\dagger \hat{c}_{j\bar{\sigma}} \hat{c}_{j\sigma}$, is included, and U is taken as $U' + 2J$ in order to keep the rotational symmetry for $M = 3$, one can repeat the previous arguments and show that $V_{eff,i\sigma}^A$ in equation (20) is still valid, changing only the last two terms by

$(1 - F_3)J(\mathcal{N}_{\bar{\sigma}} + 2n_{i\bar{\sigma}}) + F_4J(M + 2)$. The point to realize is that this change is associated with the modification of the energy gap, $[E(M + 1) - E(M)]$, that in the new Hamiltonian is $U + (M - 1)J = U' + (M + 1)J$, while in the case $U = U' + J$ takes the value $U + (M - 1)J = U' + MJ$. This suggests that both Hamiltonians yield the same $V_{eff,i\sigma}^A$ if we use parameters $\tilde{U}, \tilde{U}', \tilde{J}$ for the new case such that $\tilde{U}' - \tilde{J} = U' - J$ and $\tilde{U}' + (M + 1)\tilde{J} = U' + MJ$, an equivalency that we have checked numerically. We conclude that eq. (20) is quite general, adjusting appropriately the last two terms to the value of $[E(M + 1) - E(M)]$ as given by the corresponding model Hamiltonian.

U/T	4	6	8	12	16	32	64
f_1	(0.65) 0.55	(0.70) 0.68	(0.80) 0.71	(0.83) 0.69	(0.92) 0.71	(0.88) 0.76	(0.94) 0.82
f_2	(0.00) 0.00	(0.05) 0.03	(0.10) 0.09	(0.14) 0.17	(0.31) 0.33	(0.55) 0.61	(0.76) 0.80
f_3	0.15	0.20	0.24	0.37	0.67	0.91	1.0
α_1	(10.3) 10.1	(10.5) 11.2	(11.8) 12.3	(15.4) 17.9	(16.7) 22.4	(27.8) 45.3	(62.0) 71.7
α_2	(0.01) 0.08	(0.3) 0.4	(2.6) 4.7	(5.7) 8.2	(9.7) 13.5	(22.6) 25.1	(40.9) 36.6
α_3	25.2	41.2	48.7	63.4	78.5	87.3	165.5
α_4	17.5	24.2	36.6	39.3	44.2	55.7	167.2

TABLE II: Same as Table I for $M = 3$, $m = 1$.

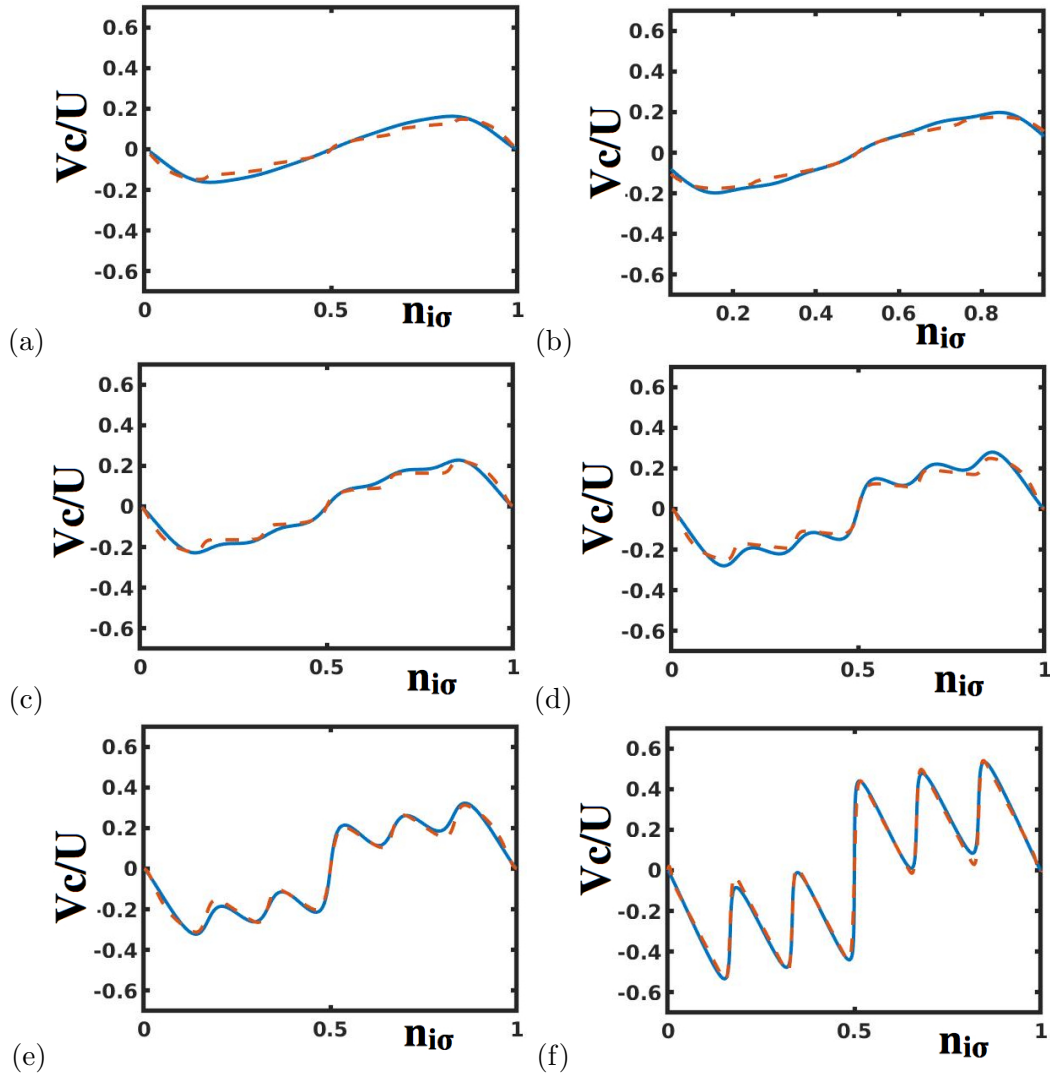


FIG. 10: (Color online) Same as Figure 6 for $M = 3$, $m = 1$.

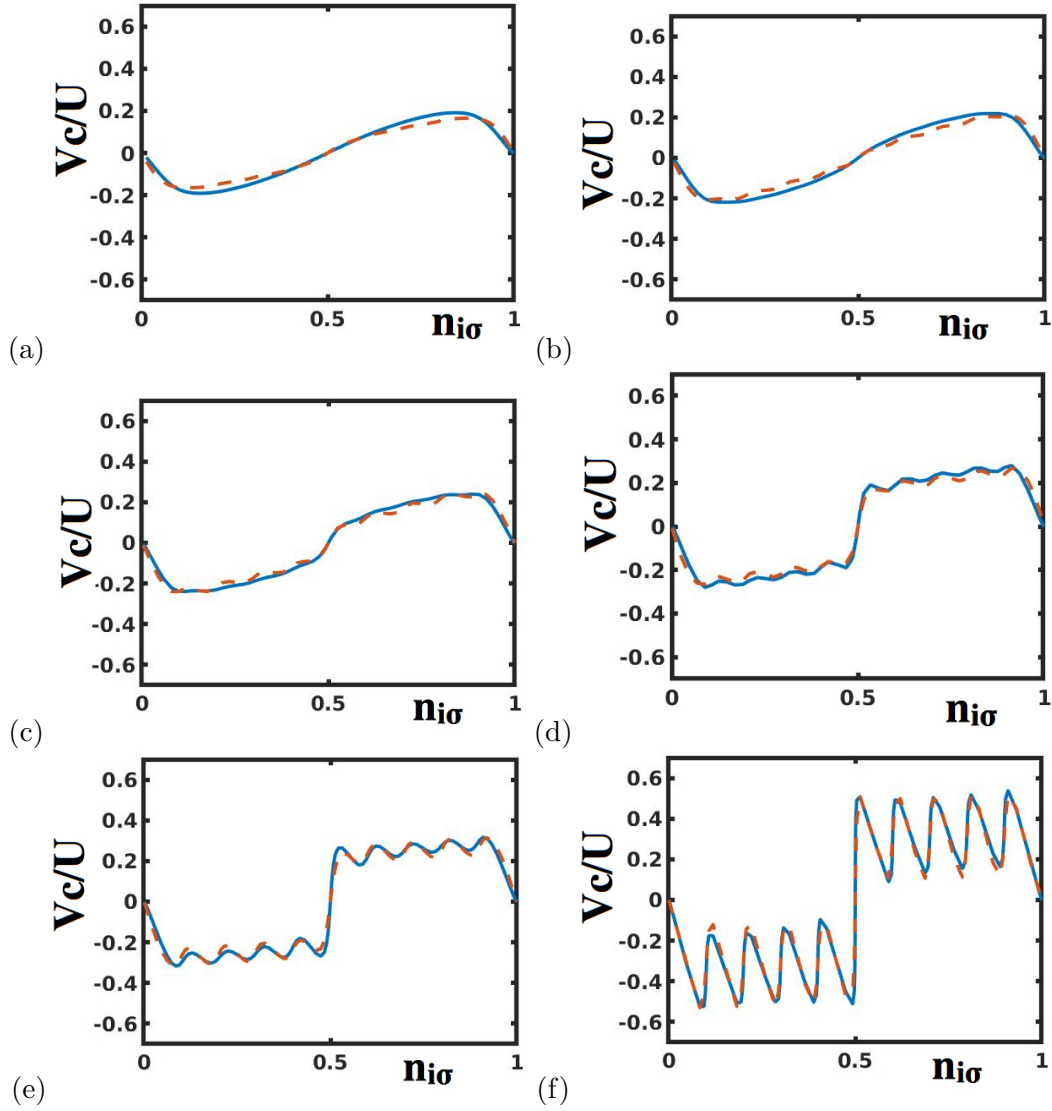


FIG. 11: (Color online) Same as Figure 6 for $M = 5$, $m = 1$.

U/T	4	6	8	12	16	32	64
f_1	(0.66) 0.57	(0.73) 0.70	(0.82) 0.73	(0.86) 0.70	(0.88) 0.72	(0.94) 0.79	(0.96) 0.82
f_2	(0.02) 0.01	(0.09) 0.09	(0.19) 0.17	(0.30) 0.32	(0.44) 0.51	(0.62) 0.66	(0.84) 0.93
f_3	0.15	0.21	0.33	0.54	0.74	0.99	1.0
α_1	(11.7) 12.1	(13.7) 22.1	(14.4) 27.2	(19.1) 34.2	(26.4) 41.8	(38.3) 87.6	(63.7) 78.6
α_2	(0.01) 0.08	(0.3) 0.3	(4.6) 5.1	(9.2) 7.5	(10.5) 19.7	(25.4) 27.5	(35.3) 38.4
α_3	25.2	41.2	48.7	63.4	78.5	87.3	165.5
α_4	11.3	14.0	31.5	47.3	48.6	154.8	291.6

TABLE III: Same as Table I for $M = 5$, $m = 1$.

D. DFT+U

The previous analysis can be used to derive a DFT+U potential appropriate for a magnetic atom within an environment as described by the model system shown in Figure 1. For this purpose we introduce the effective potential associated with the double counting energy, E_{DFT}^{dc} , which is already included in the DFT-calculation. Different double counting contributions have been proposed in the literature [40], however here for the sake of simplicity we follow Lichtenstein *et al.* [13] and define:

$$E_{DFT}^{dc} = \frac{1}{2}U'\mathcal{N}(\mathcal{N}-1) - \frac{1}{2}J\mathcal{N}_{\uparrow}(\mathcal{N}_{\uparrow}-1) - \frac{1}{2}J\mathcal{N}_{\downarrow}(\mathcal{N}_{\downarrow}-1),$$

where the Coulomb interaction between electrons is approximated by $\frac{1}{2}U'\mathcal{N}(\mathcal{N}-1)$, and the exchange interaction is given by $\frac{1}{2}J\mathcal{N}_{\uparrow}(\mathcal{N}_{\uparrow}-1) + \frac{1}{2}J\mathcal{N}_{\downarrow}(\mathcal{N}_{\downarrow}-1)$. Then, the double counting energy associated with a spin-independent DFT calculation is obtained by taking $\mathcal{N}_{\uparrow} = \mathcal{N}_{\downarrow} = \mathcal{N}/2$, so that:

$$E_{DFT}^{dc} = \frac{1}{2}U'\mathcal{N}(\mathcal{N}-1) - \frac{1}{4}J\mathcal{N}(\mathcal{N}-2).$$

Combining eq. (20) with $V_{DFT}^{dc} = (U' - J)(\mathcal{N} - \frac{1}{2}) + \frac{1}{2}J\mathcal{N}$, leads to the following DFT+U potential:

$$V_{DFT+U,i\sigma} = (1 - F_1)(U' - J) \left(\frac{1}{2} - n_{i\sigma} \right) + F_2(U' - J) \left(\frac{1}{2} - \delta\mathcal{N} \right) + (1 - F_3)J(\mathcal{N}_{\bar{\sigma}} + n_{i\bar{\sigma}}) - \frac{1}{2}J\mathcal{N} + F_4J(M+1). \quad (22)$$

The first term, $(1 - F_1)(U' - J)(1/2 - n_{i\sigma})$, represents the conventional DFT+U potential with $(U' - J)$ instead of U , *screened by* $(1 - F_1)$, while the term $F_2(U' - J) \left(\frac{1}{2} - \delta\mathcal{N} \right)$ is associated with the jump $(U' - J)$ in the atomic levels. The following exchange terms proportional to J , are dominated by $(1 - F_3)J(\mathcal{N}_{\bar{\sigma}} + n_{i\bar{\sigma}})$; it represents the exchange potential interaction screened by $(1 - F_3)$, that tends to favor magnetic solutions of the atom because for $\delta n_{i\sigma} = -\delta n_{i\bar{\sigma}} > 0$, $\delta V_{i\sigma} < 0$, this shift increasing the atomic magnetization.

It should be mentioned that in the limit $U/T \rightarrow 0$, with $F_1 \simeq F_2 \simeq F_3 \simeq F_4 \rightarrow 0$, with no correlation effect, the resulting DFT+U potential has already been described in the seminal work of Anisimov *et al.* [10, 11], using a mean field approximation for the Hubbard Hamiltonian. Our work shows how those contributions are modified by going beyond that mean field solution.

Let us now apply previous arguments to two cases that have been abundantly discussed in the literature: 3d-transition metal oxides, MnO, FeO, CoO and NiO, and metal Fe. For the 3d-metal oxides Anisimov *et al* [10] have calculated, using a constrained LDA-approach, values of U' around 7.5 eV and J around 0.9 eV; the Density of States (DOS) for these materials [11, 19] yield bandwidths, Δ , in the order of 4.5 eV. From this value, we can calculate the effective hopping, T , for the channels of Figure 1, using the equation $T = \Delta/\sqrt{12}$ given by Desjonqueres and Spanjaard [41]. These values lead to the following quantity: $U'/T = 5.8$; for $M = 5$, we find that $F_1 \simeq 0.7$, $F_2 \simeq 0.1$ and $F_3 \simeq 0.2$. Then equation (22) indicates that $(U' - J) = 6.6$ eV is screened to 2.0 eV, while J is slightly changed to 0.7 eV. These results are in good agreement with GGA+U calculations [19] that have suggested that in that approach $(U' - J)$ should be reduced to an effective value of around 3 eV in order to obtain a good density of states for these 3d-metal oxides. Metal Fe represents a similar case, because constrained LDA calculations [11] lead to $U' = 6$ eV; in metal Fe, Δ is around 4 eV, a value that leads to U'/T around 5.5. As in the previous case, this quantity indicates that $(U' - J)$ is screened to 1.8 eV, in good agreement with the effective value of U , around 2.2 eV, calculated by Cococcioni and Gironcoli [40] using a 'linear response' approach.

These two examples show that in the DFT+U calculations of the 3d-transition metal crystals, $(U' - J)(1/2 - n_{i\sigma})$, in equation (22), is much more strongly screened than the Hubbard-Hund term, $J(\mathcal{N}_{\bar{\sigma}} + n_{i\bar{\sigma}})$. This result suggests that this Hubbard-Hund term might be the dominant contribution in the formation of the atomic magnetism [43].

V. CONCLUSIONS.

In conclusion, we have presented a fully consistent many-body solution of a magnetic atom linked to different channels, as described by a Kanamori Hamiltonian, within a Density Functional formulation using as independent variables the occupation numbers $n_{i\sigma}$ of the atomic orbitals, instead of the conventional electron local density, $n_{\sigma}(\vec{r})$. In our approach, we obtain a general expression for the many-body correlation energy and the effective potential as a function of $n_{i\sigma}$, and the total number of electrons in the atom, \mathcal{N} , as well as some parameters that depend on the interaction of the atom with the environment, see eq. (20) and Tables I-III. In our analysis we first discuss the case of two atomic orbitals ($M = 2$), each one linked to a chain of three levels ($m = 3$); for this case, we have checked that using only one site for each channel ($m = 1$) yields a good approximation to the case $m = 3$. Accordingly, the $M = 3$ and $M = 5$ cases have been analyzed with one site for each channel ($m = 1$). Once the effective potential, $V_{eff,i\sigma}^A$, eq. (20), is determined for our model system, this result can be used to define a DFT+U potential in which the electron correlation effects for the magnetic atom are included in detail. The resulting DFT+U potential, V_{DFT+U} , shows how its different contributions are screened by correlation effects: interestingly, we find that the effective Coulomb interaction, $U' - J$, is more strongly screened than the exchange one, this effect indicating that the Hund rule plays a dominant role in the formation of magnetism in transition metal atoms [43].

Our solution also shows that $V_{corr,i\sigma}^A$ (or equivalently $V_{DFT+U,i\sigma}$) presents for both the Hubbard and the Hubbard-Hund cases terms like $F_2 U(1/2 - \delta\mathcal{N})$ (equation 12) or $F_2(U' - J)(1/2 - \delta\mathcal{N})$ (equation 16) reminiscent of the atomic levels (see Figures 3 and 7). In the Hubbard-Hund case an equivalent contribution is associated with the difference of energy between the central levels of the atom (for $M = 2$, $U' + 2J$, see Figure 7). These contributions are relevant for $U/T \geq 6$ and, accordingly, one might wonder if these new terms, having an atomic flavour, would offer a possibility for obtaining, within the DFT+U approach and for large U/T , the Mott insulating ground state of a paramagnetic system. The answer is negative since, as argued in references [9, 44], one can say that any local potential can never create that Mott-like energy gap unless the system is "prepared" by introducing a broken symmetry, either in the spin or in the orbitals.

However, the new DFT+U potential introduced in this paper might present advantages

1
2
3
4
5
6
7
8
9
10
11
12
13
14
15
16
17
18
19
20
21
22
23
24
25
26
27
28
29
30
31
32
33
34
35
36
37
38
39
40
41
42
43
44
45
46
47
48
49
50
51
52
53
54
55
56
57
58
59
60

for calculating more "exact" solutions of those "prepared" systems for which an energy gap can be calculated; the main reason behind this expectation is that by having an improved correlation potential one could obtain a better description of how the electronic charge is distributed among the electrons of the magnetic atom.

Acknowledgements

This work was funded by Spanish Ministry of Science and Innovation under projects No. MAT2017-88258-R and No. CEX2018-000805-M (María de Maeztu Programme for Units of Excellence in R&D).

VI. APPENDIX A.1

In this appendix we also present the correlation energy, $E_{corr}^A(n_{i,\sigma})$ for the different cases considered in Figs. 2, 6, 10 and 11. In all these cases $V_{corr,i\sigma}^A = \frac{\partial E_{corr}^A(n_{i,\sigma})}{\partial n_{i,\sigma}}$, where $n_{i\sigma} = \mathcal{N}/2M$, see also ref. [32]. For very small values of U/T ($U/T \ll 4$), $E_{corr}^A(n_{i,\sigma})$ behaves as $\sim U^2/Tn_{i\sigma}^2(1-n_{i\sigma})^2$ in the Hubbard case or as $\sim (U' - J)^2/Tn_{i\sigma}^2(1-n_{i\sigma})^2$ in the Hubbard-Hund case.

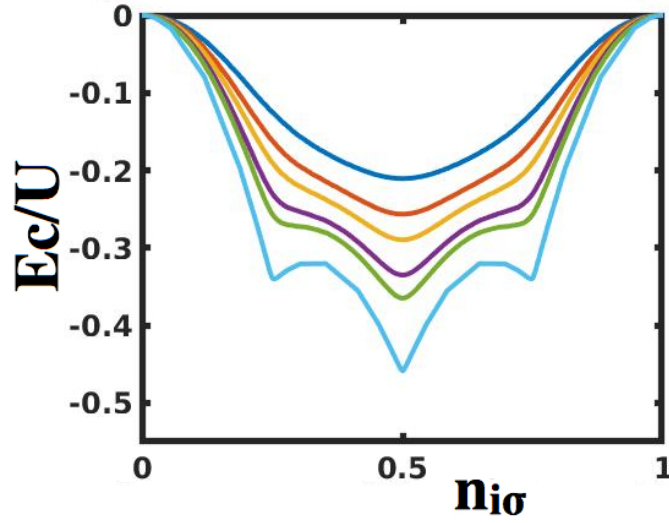


FIG. 12: (Color online) $E_{corr}^A(n_{i,\sigma})$ in units of U for the Hubbard case, $J = 0$, $M = 2$ and $m = 3$, and different values of $U/T = 4, 6, 8, 12, 16, 64$ (top to bottom).

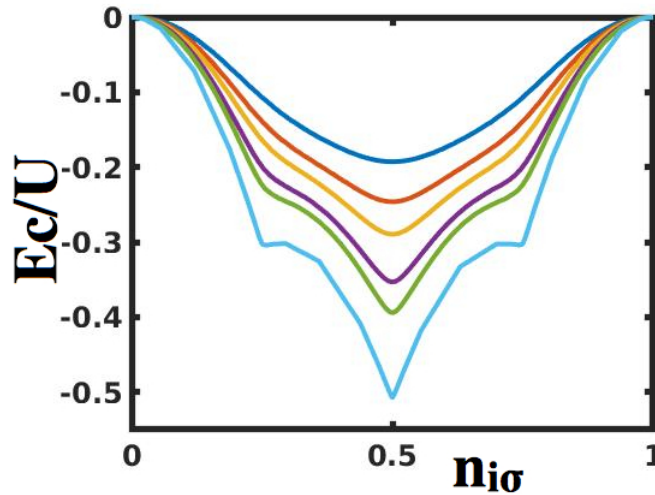


FIG. 13: (Color online) As Figure 12 for the Hubbard-Hund case, $J = 0.1$

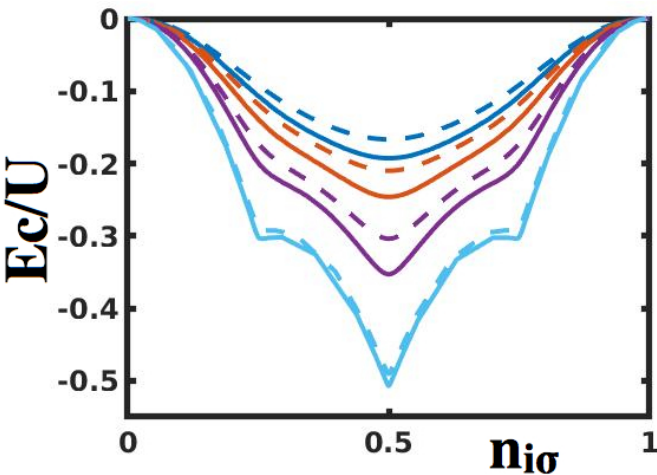


FIG. 14: (Color online) Comparison of $E_{corr}^A(n_{i,\sigma})$ in units of U for the Hubbard-Hund case, $J = 0.1U$, $M = 2$ and $m = 3$ (solid lines) and $m = 1$ (dashed lines) and different values of $U/T = 4, 6, 12, 64$ (top to bottom).

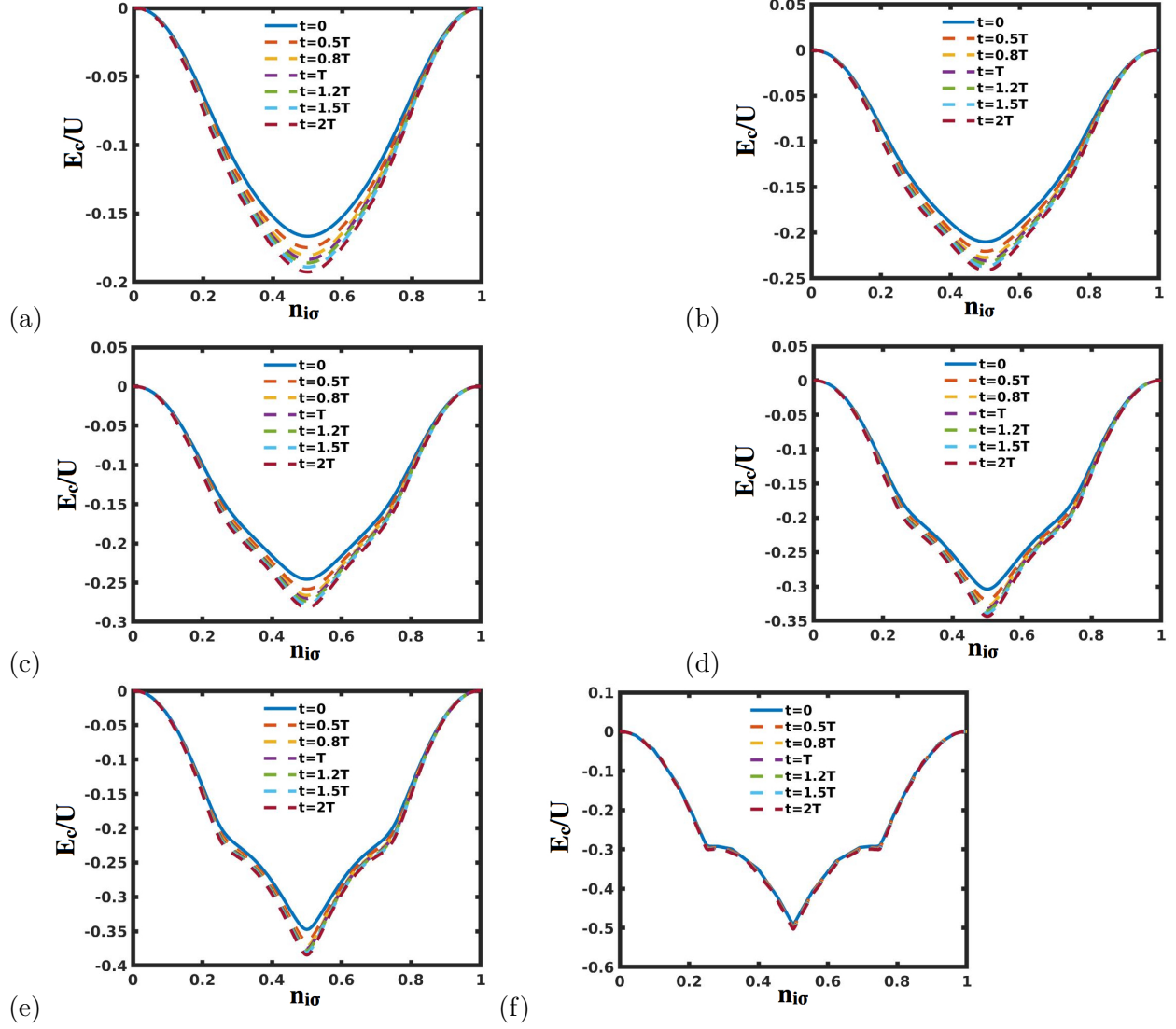


FIG. 15: Correlation energy as a function of $n_{i\sigma}$ in units of U in the Hubbard-Hund case ($J = 0.1U$) for different values of t between 0 and $2T$, for $U/T = 4, 6, 8, 12, 16, 64$, and $M = 2, m = 3$. The solid blue line ($t = 0$) corresponds to the $M = 2, m = 1$ case.

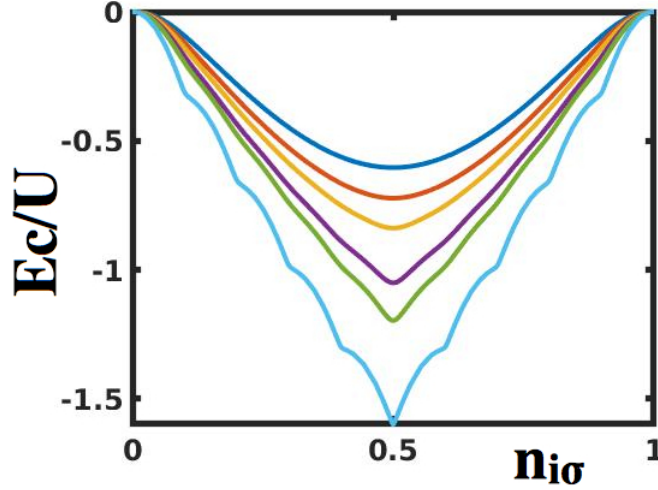


FIG. 16: (Color online) $E_{corr}^A(n_{i,\sigma})$ in units of U for the Hubbard-Hund case, $J = 0.1U$, $M = 5$ and $m = 1$, and different values of $U/T = 4, 6, 8, 12, 16, 64$ (top to bottom).

VII. APPENDIX A.2

In this section we represent $V_{eff}^A(n_{i,\sigma})$ for the Hubbard-Hund case and $M = 3$ (Fig. 17) or $M = 5$ (Fig. 19). In Fig. 18 we represent the jump between atomic levels in the Hubbard-Hund case for three atomic orbitals ($M = 3$), analogously to fig. 7.

It is interesting to realize that $V_{eff,i\sigma}^A$ is practically a straight line for $U/T \leq 6$ for $M = 3$ or 5 except for a small bending $n_{i,\sigma}$ near 0 or 1; even for $U/T = 8$ we find only small kinks around $n_{i,\sigma} \approx 0.5$. This reinforces our comment that $V_{eff,i\sigma}^A$ can be well approximated by eq. (21) for $U/T \leq 6$.

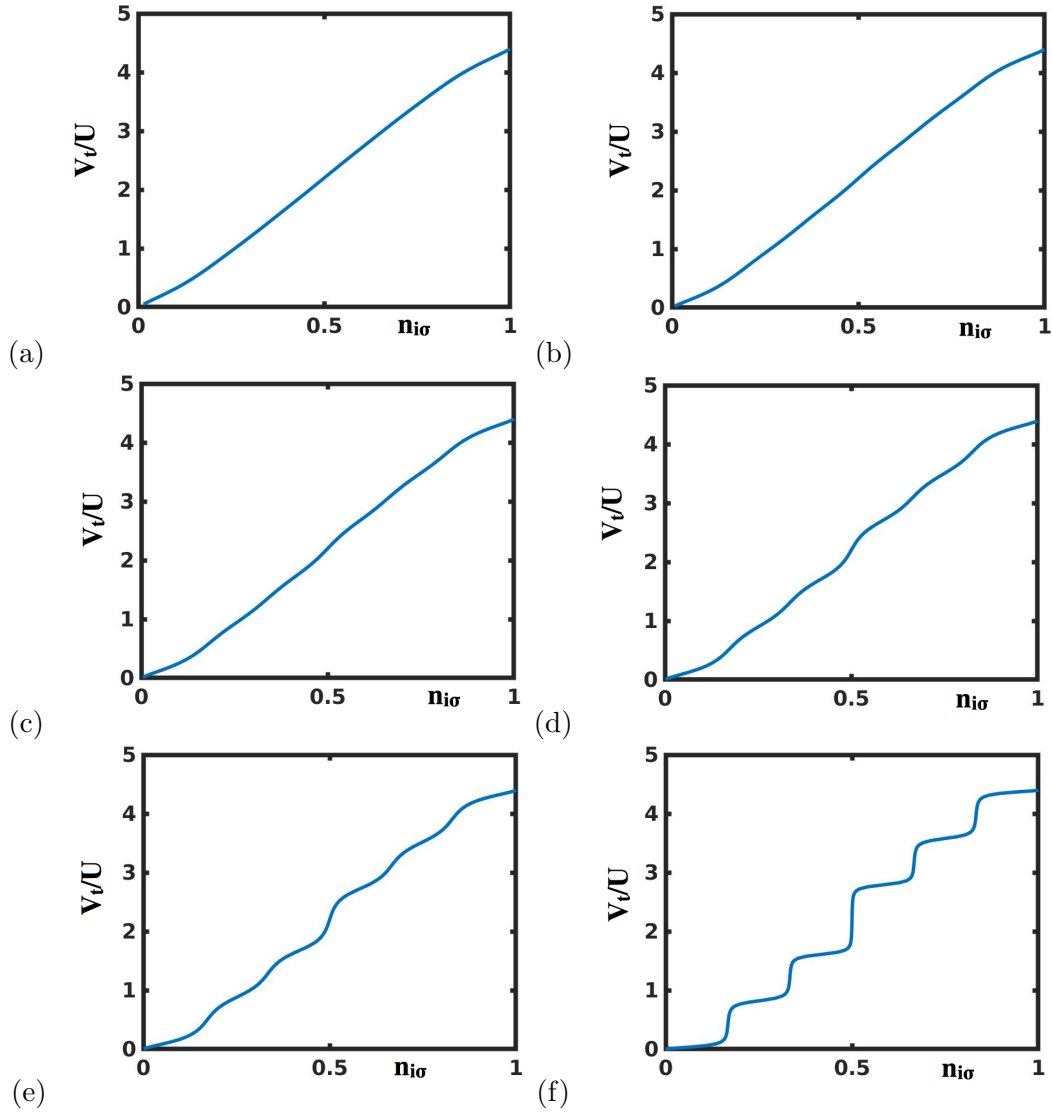


FIG. 17: Effective potential, $V_{eff,i\sigma}^A$, in units of U for the Hubbard-Hund case ($J = 0.1U$), for $M = 3$, $m = 1$ and $U/T = 4, 6, 8, 12, 16, 64$.

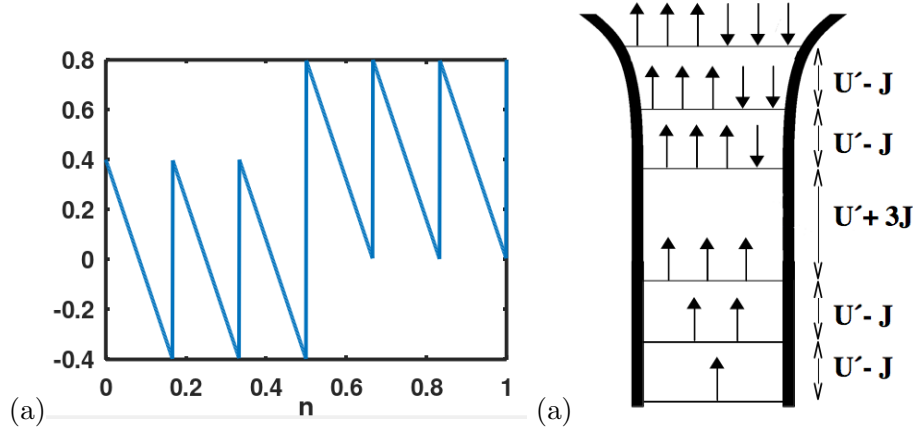


FIG. 18: (a) Sawtooth behaviour of $(U' - J) \left(\frac{1}{2} - \delta N \right) + J(M + 1)\Theta(N - M)$, see equations (15) and (19), in units of U for $M = 3$; (b) Atomic levels, $E^A(N) - E^A(N - 1) = 0, U' - J, 2(U' - J), 3U' + J, 4U', 5U' - J$ for different atomic charges, $N = 1, 2, 3, 4, 5, 6$. The jump between the levels for four and three electrons, $U' + 3J$ is reflected in the jump in (a) for $n_{i\sigma} = 0.5$.

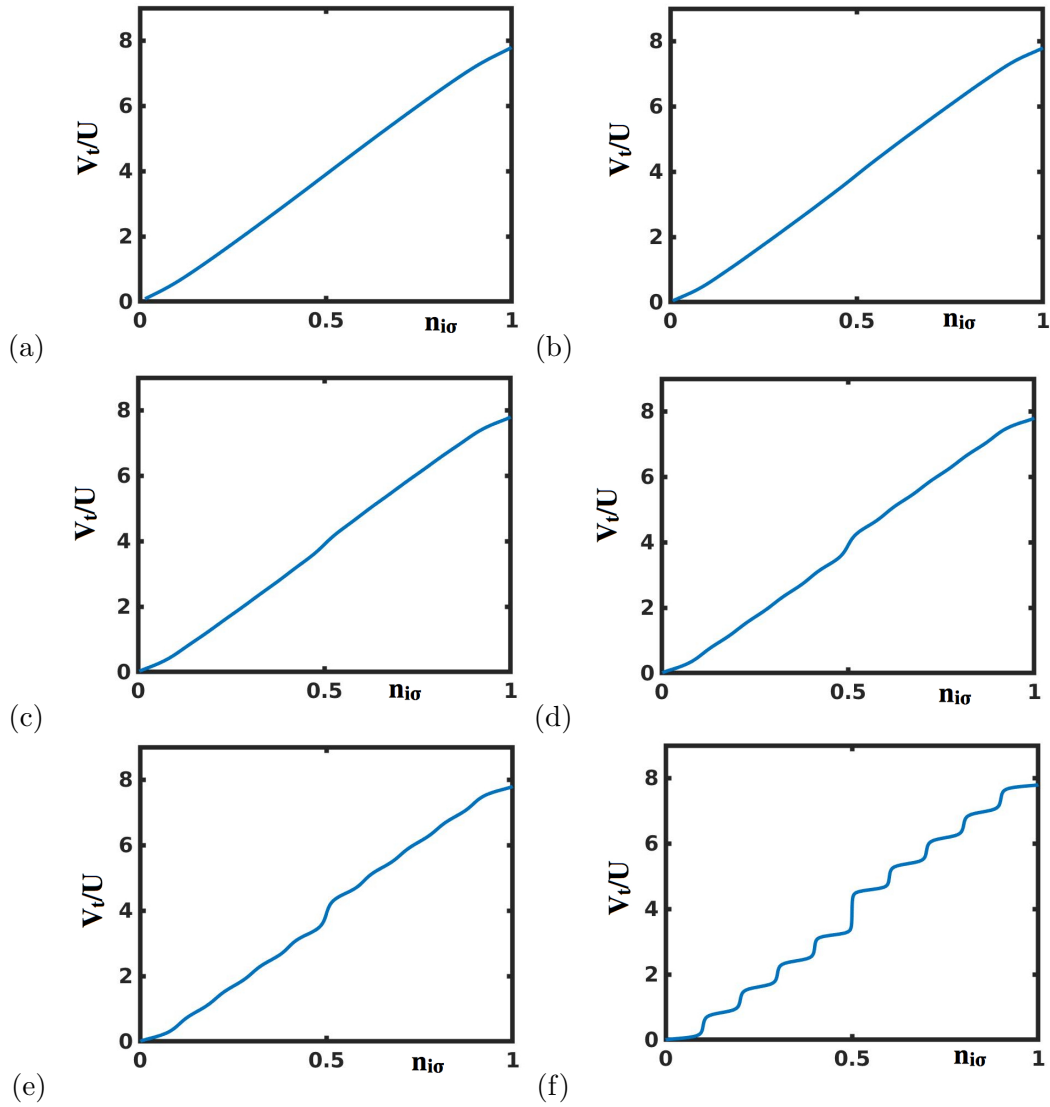


FIG. 19: Effective potential, $V_{eff,i\sigma}^A$ in units of U , for the Hubbard-Hund case ($J = 0.1U$) for $M = 5$, $m = 1$ and $U/T=4, 6, 8, 12, 16, 64$.

VIII. APPENDIX A.3

$\hat{c}_{i\sigma}^\dagger / \hat{c}_{i\sigma}$	creation/annihilation operator of the i -th level with spin σ in the atom
$\hat{c}_{j\alpha\sigma}^\dagger / \hat{c}_{j\alpha\sigma}$	creation/annihilation operator of the α -th level of the j -th chain with spin σ , see equation 3.
$\hat{c}_{\alpha\sigma}^\dagger / \hat{c}_{\alpha\sigma}$	generic creation/annihilation operator in the theoretical discussion in section III.
$\hat{n}_{i\sigma}$	Number operator in the i -th level of the atom with spin σ , $\hat{c}_{i\sigma}^\dagger \hat{c}_{i\sigma}$
$n_{i\sigma}$	$\langle \hat{c}_{i\sigma}^\dagger \hat{c}_{i\sigma} \rangle$, that is, occupation of the i -th atomic level with spin σ .
\mathcal{N}	Total number of electrons in the atom: $\mathcal{N} = \sum_{i\sigma} n_{i\sigma}$.
N	Floor function of \mathcal{N} (i.e., greatest integer number smaller than \mathcal{N})
$\delta\mathcal{N}$	Fractional part of \mathcal{N} , i.e: $\delta\mathcal{N} = \mathcal{N} - N$
f_j	Screening parameters of the different contributions to the correlation potentials
α_j	Width of the hyperbolic tangents in eqs. 13.
F_j	Product of the f_j and the corresponding tanh, e.g $F_1 = f_1 \tanh(\alpha_1 n_{i\sigma}(1 - n_{i\sigma}))$ etc.
Θ	The Heaviside step function.
M	Number of i -orbitals in the atom; the number of $i\sigma$ -orbitals is $2M$ (see Figs. 1 and 3)
m	Number of levels in the chain connected to each atomic level (see Fig. 1)

-
- [1] P. Hohenberg and W. Kohn, *Physical Review* **136**, B864 (1964).
- [2] W. Kohn and L. J. Sham, *Physical Review* **140**, A1133 (1965).
- [3] E. Gross and R. Dreizler, *Density Functional Theory* (Springer-Verlag, 1990).
- [4] W. Kohn, *Rev. Mod. Phys.* **71**, 1253 (1998).
- [5] W. Koch M. C. Holthausen, *A Chemist's Guide to Density Functional Theory* (Wiley-VCH, 2000).
- [6] J. P. Perdew, R. G. Parr, M. Levy, and J. L. Balduz, *Physical Review Letters* **49**, 1691 (1982).
- [7] L. Hedin, *Physical Review* **139**, A796 (1965).
- [8] M. S. Hybertsen and S. G. Louie, *Physical Review B* **34**, 5390 (1986).
- [9] G. Kotliar, S. Y. Savrasov, K. Haule, V. S. Oudovenko, O. Parcollet, and C. A. Marianetti, *Reviews of Modern Physics* **78**, 865 (2006).
- [10] V. I. Anisimov and O. Gunnarsson, *Physical Review B* **43**, 7570 (1991).
- [11] V. I. Anisimov, J. Zaanen, and O. K. Andersen, *Physical Review B* **44**, 943 (1991).
- [12] I. V. Solovyev, P. H. Dederichs, and V. I. Anisimov, *Physical Review B* **50**, 16861 (1994).
- [13] A. I. Liechtenstein, V. I. Anisimov, and J. Zaanen, *Physical Review B* **52**, R5467 (1995).
- [14] V. I. Anisimov, F. Aryasetiawan, and A. I. Liechtenstein, *Journal of Physics: Condensed Matter* **9**, 767 (1997).
- [15] S. L. Dudarev, P. Liu, D. A. Andersson, C. R. Stanek, T. Ozaki, and C. Franchini, *Physical Review Materials* **3**, 83802 (2019).
- [16] L. A. Agapito, S. Curtarolo, and M. Buongiorno Nardelli, *Phys. Rev. X* **5**, 011006 (2015).
- [17] D. A. Scherlis, M. Cococcioni, P. Sit, and N. Marzari, *The Journal of Physical Chemistry B* **111**, 7384 (2007).
- [18] M. Shishkin and H. Sato, *Journal of Chemical Physics* **151**, 164124 (2019).
- [19] C. Rödl, F. Fuchs, J. Furthmüller, and F. Bechstedt, *Physical Review B* **79**, 235114 (2009).
- [20] B. Himmetoglu, A. Floris, S. De Gironcoli, and M. Cococcioni, *International Journal of Quantum Chemistry* **114**, 14 (2014).
- [21] Y. Bi, Z. Cai, D. Zhou, Y. Tian, Q. Zhang(m), Q. Zhang(f), Y. Kuang, Y. Li, X. Sun, and X. Duan, *Journal of Catalysis* **358**, 100 (2018).
- [22] M. M. Obeid, H. R. Jappor, K. Al-Marzoki, I. A. Al-Hydary, S. J. Edrees, and M. M. Shukur,

- RSC Advances **9**, 33207 (2019).
- [23] K. Chakrapani, G. Bendt, H. Hajiyani, T. Lunkenbein, M. T. Greiner, L. Masliuk, S. Salamon, J. Landers, R. Schlögl, H. Wende, R. Pentcheva, S. Schulz, and M. Behrens, ACS Catalysis **8**, 1259 (2018).
- [24] G. Trimarchi, Z. Wang, and A. Zunger, Physical Review B **97**, 035107 (2018).
- [25] M. T. Czyzyk and G. A. Sawatzky, Physical Review B **49**, 14211 (1994).
- [26] H. J. Kulik, M. Cococcioni, D. A. Scherlis, and N. Marzari, Physical Review Letters **97**, 103001 (2006).
- [27] M. Cococcioni and S. de Gironcoli, Phys. Rev. B **71**, 035105 (2005).
- [28] N. Tancogne-Dejean and A. Rubio, Physical Review B **102**, 155117 (2020).
- [29] E. B. Linscott, D. J. Cole, M. C. Payne, and D. D. O'Regan, Physical Review B **98**, 235157 (2018).
- [30] S. Keshavarz, J. Schött, A. J. Millis, and Y. O. Kvashnin, Physical Review B **97**, 184404 (2018).
- [31] F. J. García-Vidal, J. Merino, R. Pérez, R. Rincón, J. Ortega, and F. Flores, Physical Review B **50**, 10537 (1994).
- [32] P. Pou, R. Pérez, F. Flores, A. L. Yeyati, A. Martin-Rodero, J. Blanco, F. García-Vidal, and J. Ortega, Physical Review B - Condensed Matter and Materials Physics **62**, 4309 (2000).
- [33] J. Kanamori, Progress of Theoretical Physics **30**, 275 (1963).
- [34] A. Georges, L. De Medici, and J. Mravlje, Annual Review of Condensed Matter Physics **4**, 137 (2013).
- [35] A. Horvat, R. Žitko, and J. Mravlje, Physical Review B **94**, 165140 (2016).
- [36] B. Himmetoglu, R. M. Wentzcovitch, and M. Cococcioni, Phys. Rev. B **84**, 115108 (2011).
- [37] O. K. Orhan and D. D. O'Regan, Phys. Rev. B **101**, 245137 (2020).
- [38] E. R. Ylvisaker, W. E. Pickett, and K. Koepf, Phys. Rev. B **79**, 035103 (2009).
- [39] E. Pavarini, in *The LDA+DMFT approach to strongly correlated materials* (Forschungszentrum Jülich GmbH Institute for Advanced Simulations, 2014) Chap. The LDA+DMFT Approach, pp. 321–341.
- [40] M. Cococcioni, Theoretical and Computational Methods in Mineral Physics: Geophysical Applications **71**, 147 (2018).
- [41] D. Desjonqueres; C. Spanjaard, in *Interaction of Atoms and Molecules with Solid Surfaces*,

edited by V. Bortolani et al. (Springer-Verlag, 1990) Chap. Electronic Theory of Chemisorption, pp. 255–323.

- [42] K. Schönhammer, O. Gunnarsson, and R. M. Noack, *Physical Review B* **52**, 2504 (1995).
- [43] P. Pou, F. Flores, J. Ortega, R. Pérez, and A. L. Yeyati, *Journal of Physics Condensed Matter* **14**, L421–L427 (2002).
- [44] M. Cococcioni and S. De Gironcoli, *Physical Review B - Condensed Matter and Materials Physics* **71**, 1 (2005).